Expression profile of plakin crosslinking proteins in denervated skeletal muscle of mice

By

Patrick Blouin

Thesis submitted in partial fulfillment
of the requirements for the degree of
Master of Human Kinetics (MHK)

School of Graduate Studies
Laurentian University
Sudbury, Ontario

THESIS DEFENCE COMMITTEE/COMITÉ DE SOUTENANCE DE THÈSE
Laurentian Université/Université Laurentienne
Faculty of Graduate Studies/Faculté des études supérieures

Title of Thesis Titre de la thèse	Plakin expression in denervated mouse hind limb skeletal muscle	
Name of Candidate Nom du candidat	Blouin, Patrick	
Degree Diplôme	Master of Science	
Department/Program Département/Programme	Human Kinetics	Date of Defence Date de la soutenance septembre 16, 2015

APPROVED/APPROUVÉ

Thesis Examiners/Examinateurs de thèse:

Dr. Celine Lariviere
(Supervisor/Directeur(trice) de thèse)

Dr. Olivier Serresse
(Committee member/Membre du comité)

Dr. Sandra Dorman
(Committee member/Membre du comité)

Approved for the Faculty of Graduate Studies
Approuvé pour la Faculté des études supérieures
Dr. David Lesbarrères
Monsieur David Lesbarrères

Dr. Simon Lees Acting Dean, Faculty of Graduate Studies
(External Examiner/Examinateur externe)

Doyen intérimaire, Faculté des études supérieures

ACCESSIBILITY CLAUSE AND PERMISSION TO USE

I, **Patrick Blouin**, hereby grant to Laurentian University and/or its agents the non-exclusive license to archive and make accessible my thesis, dissertation, or project report in whole or in part in all forms of media, now or for the duration of my copyright ownership. I retain all other ownership rights to the copyright of the thesis, dissertation or project report. I also reserve the right to use in future works (such as articles or books) all or part of this thesis, dissertation, or project report. I further agree that permission for copying of this thesis in any manner, in whole or in part, for scholarly purposes may be granted by the professor or professors who supervised my thesis work or, in their absence, by the Head of the Department in which my thesis work was done. It is understood that any copying or publication or use of this thesis or parts thereof for financial gain shall not be allowed without my written permission. It is also understood that this copy is being made available in this form by the authority of the copyright owner solely for the purpose of private study and research and may not be copied or reproduced except as permitted by the copyright laws without written authority from the copyright owner.

Abstract

Plakin crosslinking proteins are important structural elements that are expressed in many animal tissues, especially those which require resistance to mechanical stress. The three plakin proteins most prevalent in skeletal muscle are plectin, dystonin and microtubule-actin crosslinking factor (MACF). Skeletal muscle atrophy linked to inactivity is a complex phenomenon involving widespread alteration of muscle physiology, often characterized by expression of normally repressed embryonic genes in adult muscle. We investigate the response of the plakins: plectin, dystonin and MACF to denervation-induced atrophy in mice. We found that MACF, which is expressed more abundantly during embryonic development, is upregulated following denervation both at the mRNA and protein level as assessed using qPCR and western blotting. Plectin and dystonin were both downregulated at the mRNA level but remained constant or even upregulated at the protein level, indicating their potential importance in the baseline preservation of the skeletal muscle structure following denervation-induced atrophy.

Keywords:

Plakin, plectin, dystonin, MACF, denervation, atrophy

Acknowledgements

The following people deserve my thanks.

My advisor, Dr. Céline Larivière, for assistance in the lab, her continued guidance and her patience during my procrastination. You are living up to the standard set by your coffee mug.

My committee members, Dr. Sandra Dorman and Dr. Olivier Serresse, for valuable advice during the planning phase of the experiments and in the reviewing phase of my thesis.

Paul Michael, who was always willing to put aside his own work to help not only me but everyone else in the lab. My experiments would not have succeeded without your help, and the entire lab would be in a lot of trouble without you.

My family for their support during my studies, both graduate and undergraduate.

And finally my girlfriend, Lyndsey, for dealing with my less-than-enjoyable self during the occasional times of stress during the past three years of graduate studies and the four years of undergraduate studies before that.

Table of Contents

List of Figures

List of Tables

List of Appendices

List of Abbreviations

AChE; Acetylcholinesterase
AChR; Acetylcholine receptor
ANOVA; Analysis of variance
ATP; Adenosine triphosphate
CH; calponin homology
cDNA; Complementary DNA
Den; Denervated
DGP; Dystrophin glycoprotein complex
dt; Dystonia musculorum
dt^{Tg4}; Dystonia musculorum transgenic line 4 (insertional mutation)
ECM; Extracellular matrix
GAS2; Growth arrest specific 2
HDAC4; Histone deacetylase 4
IF; Intermediate filament
IFBD; Intermediate filament binding domain
IFBD2; Intermediate filament binding domain of the dystonin-b muscle isoform
MACF; Microtubule actin cross-linking factor
MuRF1; Muscle ring finger 1
mdx; Dystonia Musculorum mouse model
MF; Microfilaments
MHC; Myosin heavy chain
MLC; Myosin light chain
mRNA; Messenger RNA
MT; Microtubules
nAChR; Nicotinic acetylcholine receptor
NMJ; Neuromuscular junction
PCR; Polymerase chain reaction
PRD; Plakin repeat domain
qPCR; Quantitative polymerase chain reaction
RNA; Ribonucleic acid
RNAi; RNA interference
Sham; Sham-denervated (control procedure)
wt; Wild-type

Chapter 1

1. Introduction

Voluntary movement is one of the key elements which differentiate animals (*Kingdom Animalia*) from other organisms such as plants (*Kingdom Plantae*) (Slack et al. 1993). In mammals, including humans, skeletal muscle, through its close interaction with the somatic nervous system, converts energy into movement (MacIntosh et al. 2006). Complex physiological processes underlie proper muscle function and it is vital to understand these mechanisms, as they shed light on skeletal muscle adaptability. The structure and function of skeletal muscle are altered in various movement-impairing pathologies, which can affect the ability of people to carry out their activities of daily life (Mitchell et al. 2012; Kharraz et al. 2014; Chatzifrangkeskou et al. 2015). At the other end of the spectrum, skeletal muscle tissue is known to change its phenotype in response to exercise and this is especially important in the case of athletic/sport performance, where a good result is often intimately linked with skeletal muscle function (Timmons 2011; Phillips 2014). Understanding how muscles adapt at both ends of the spectrum of health and illness has the potential to inform training programs and therapies to optimize muscle function and movement.

1.1. Healthy skeletal muscle tissue

Skeletal muscle is an excitable tissue capable of generating force through contraction. Skeletal muscle tissue, as well as cardiac muscle, display a unique structure and subcellular organization characterized by striations; as such it is also known as 'striated muscle.' Skeletal muscle cells are multinucleated, elongated structures which contain contractile elements

known as sarcomeres. Sarcomeres are complex arrangements of multiple proteins. Actin and myosin, the main contractile proteins, are arranged with great precision and regularity. Their overlap causes the visible striations in muscle (Clark et al. 2002; MacIntosh et al. 2006). Figure 1-1, adapted from Braun & Gautel, (2011) illustrates the sarcomere. Its components will be discussed.

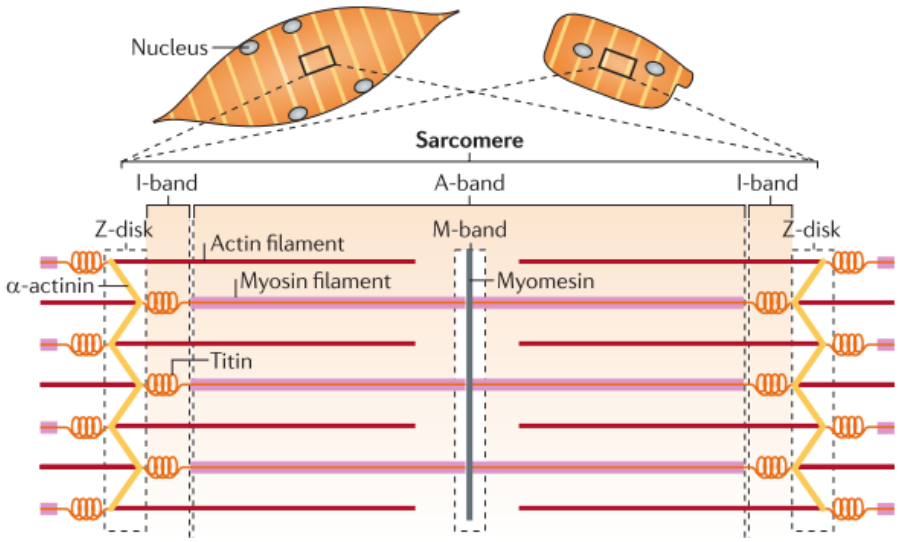

Figure 1-1: An illustration of the sarcomere, the fundamental contractile unit of muscle. Shown are the Z-disks (whose main component is α-actinin), the interaction of actin filaments and titin with the Z-disks as well as the spring-like function of titin. The M-band is also shown. In the M-band, proteins including myomesin crosslink myosin filaments near the centre of the sarcomere. Above, skeletal muscle (left) and cardiac muscle (right) are shown. They both contain sarcomeres, but their morphology is different. Skeletal muscle has peripheral nuclei whereas cardiac muscle does not (adapted from Braun & Gautel, 2011).

1.1.1. Actin filaments

Actin is expressed in all mammalian tissues, including muscle (Dominiguez & Holmes 2011). There are three main actin isoforms in vertebrates: Alpha (α)-actin, Beta (β)-actin and Gamma (γ)-actin. These isoforms organize into a protein known as globular (G)-actin. G-actin is a globular protein that is folded into two main domains (small and large) which are each divided into two subdomains, where subdomains 1 and 2 are part of the small domain and subdomains 3 and 4 are part of the large subdomain (Dominiguez & Holmes 2011). Globular actin polymerizes into a polymer known as Filamentous (F)-actin. F-actin is the protein which forms the actin filaments depicted in Figure 1-1. This long strand of actin forms a helix where approximately six turns are completed for every 13 globular actin molecules (Dominiguez & Holmes 2011).

1.1.2. Myosin filaments

Myosin filaments are polymers of myosin. There are many isoforms of myosin divided into 15 classes. The focus for this thesis will be Class II Myosins. Class II myosins are known as "conventional" myosins; they are found in muscle cells and they form filaments which hydrolyze adenosine triphosphate (ATP) to produce movement through interactions with actin (Sellers 2000). Myosin filaments are composed of subunits of two myosin heavy chains (MHC) and four myosin light chains (MLC) (Clark et al. 2002). Two of the MLCs have a regulatory function, while the second pair of MLCs is structural. The MHCs are arranged in a way as to form a separate 'head' region, where the binding sites protrude from the myosin filaments and interact with actin to initiate muscle contraction (MacIntosh et al. 2006). The remainder of the myosin molecules interact towards the center of the filament and polymerize, creating the myosin filament itself. Myosin filaments terminate at the M-band (see Figure 1-1) at the center

of the sarcomere where they interact with proteins such as myomesin to form a cohesive structure of thick myosin filaments.

1.1.3. Titin

Titin is a large protein with a molecular weight of roughly 4200kDa in humans (Bang et al. 2001). It is the largest known protein and the third most abundant protein in muscle, after actin and myosin (Clark et al. 2002). It reaches from the Z-line to the M-line and spans the entire sarcomere (Trinick & Tskhovrebova 2010). It is thought to provide structure and elastic properties to the muscle as demonstrated in Figure 1-1 where titin is depicted as a spring-like coil. This giant protein has been shown to slightly change shape under small applied forces while under large forces, the polypeptide unravels, returning to its shorter state when force is no longer applied (Trinick & Tskhovrebova 2010). When isolated outside of the sarcomere, titin does not maintain its rod shape but assumes a coiled appearance (Trinick & Tskhovrebova 2010), which indicates a certain amount of passive elasticity even when the sarcomere is at rest.

1.1.4. Z-disk proteins

The Z-disk, also known as the Z-line because when viewed as two dimensional longitudinal cross sections of muscle it appears as a line, is the limit of a sarcomere; a sarcomere spans from Z-disk to Z-disk. The Z-disk is a complex network of proteins that include α-actinin and many other proteins not shown in Figure 1-1. Alpha-actinin is the most abundant protein of the Z-disk and one of its functions is to cross-link actin filaments (Faulkner et al. 2001). Alpha-actinin also binds other proteins at the Z-disk, with structural or regulatory functions (Faulkner et al. 2001). One example is nebulin, a protein which binds to α-actinin at

its C-terminal end and its N-terminal end extends to the tips of actin filaments where it regulates actin filament length (Clark et al. 2002). Desmin, the most abundant intermediate filament in muscle, also binds to the Z-disk (Capetanaki et al. 2007).

Intermediate filaments are very important in muscle structure, but they are not part of the sarcomere. Their implication in the structural rigidity of muscle is discussed below. Filamin is another important protein which binds to α-actinin at the Z-disk and to sarcoglycans at the Dystrophin Glycoprotein complex (DGC), an important anchor site near the sarcolemma for force transduction in muscle (Clark et al. 2002). Evidently, the Z-disk is an important adhesion structure in muscle which crosslinks many important structural and regulatory proteins.

1.2. Cytoskeletal proteins and the structure of the skeletal muscle cell

Skeletal muscle cells have distinct morphology compared to other cells. One major difference is the positioning of their nuclei, which are peripherally located in mature cells (see Figure 1-1). Skeletal muscle mitochondria are also more numerous than in other cells, such as epithelial cells (Hoppeler & Fluck 2003). Mitochondria are localized in pairs adjacent to z-disks through plectin and desmin binding, but are also located between the sarcolemma and the myofibrils (Reipert et al. 1999; Picard et al. 2012); desmin intermediate filaments are important elements of the skeletal muscle cytoskeleton.

The cytoskeleton is an intricate network of large structural proteins which interact in order to provide structure to the cell. Cytoskeletal proteins are polymers that are often large enough to span the width of the entire cell (Erickson 2007). The three main components of the cytoskeleton are microtubules (tubulin subunits), microfilaments (actin subunits) and

intermediate filaments (e.g. desmin, especially in muscle). The main components of the cytoskeleton are interconnected or crosslinked by large proteins belonging to the plakin family (described below), thought to act as scaffolding proteins which solidify the cell architecture (Bouameur et al. 2014).

1.3. Plakins

Plakins are a class of cytolinker proteins which bind to various elements of the cytoskeleton but also to various organelles and cell membrane proteins. Plakins are found in all metazoa, but not in eukaryotes such as yeast (Suozzi et al. 2012). They likely evolved to fulfill specific structural roles in the cells of higher animals. *Drosophila*, or fruit flies, contain only one plakin gene, known as short stop/kakapo, which codes a small number of different isoforms through alternative splicing (Suozzi et al. 2012). In mammals such as mice and humans, there are many plakin genes coding a large number of isoforms. These include dystonin, Microtubule-Actin Crosslinking Factor (MACF), plectin, periplakin, epiplakin, envoplakin and desmoplakin (Ferrier et al. 2013). It has been postulated that plakins evolved to fulfill the need for structural integrity in highly mobile animals as their tissues have the potential to deform more than in insects. These diverse mammalian plakin isoforms may have some form of functional redundancy during developmental phases (Ferrier et al. 2013). However, many plakin mutations are lethal as demonstrated in desmoplakin knockout mice (Jefferson et al. 2004) and in VAB10-mutated *C. Elegans* (VAB10 is the plakin version of MACF in *C. Elegans*) (Bosher et al. 2003). In this sense, plakins are not always functionally redundant.

1.4. Mammalian plakin diversity

1.4.1. Plakins versus spectraplakins

Plakins evolved from proteins known as spectrins. Some plakin isoforms still contain spectrin repeat domains, which are characteristic of spectrins, but also contain plakin repeat domains. These proteins are known as spectraplakins. However, some authors have criticized this distinction because it was found that plakin repeat domains themselves evolved from spectrins and should still be characterized as spectrins (Sonnenberg & Liem 2007). This would mean that all proteins containing plakin repeat domains are spectraplakins, rendering the distinction useless. However, even if plakin repeat domains show similar sequence similarity to spectrin repeats and can be shown to be derived from spectrin repeats, they are still functionally distinct. Spectraplakins have roles not shared with plakin family proteins which have lost their spectrin repeat domains (Sonnenberg & Liem 2007). Spectraplakins can span larger distances in the cell due to the rod-like spectrin repeats which add length to the protein. Of the seven plakin proteins, only MACF and dystonin are considered spectraplakins.

1.4.2. Dystonin

The dystonin gene in mammals is a very large gene which codes a variety of proteins through alternative splicing (Leung et al. 2001). In fact, diverse plakin protein variants are produced via alternative splicing of a limited numbers of genes and not as a result of transcription of numerous genes. There are three main isoforms of dystonin: dystonin-a, dystonin-b and dystonin-e (which are neural, muscle and epithelial isoforms, respectively). Of these isoforms, there are variants of a and b with different N- or C- terminal regions producing even more complexity. For example, dystonin-a has isoform a1, a2 and a3, each with functionally distinct N-terminal regions. One N-terminal region binds to actin and another has a

transmembrane domain. The following figure from Ferrier et al. (2013) illustrates these dystonin isoforms:

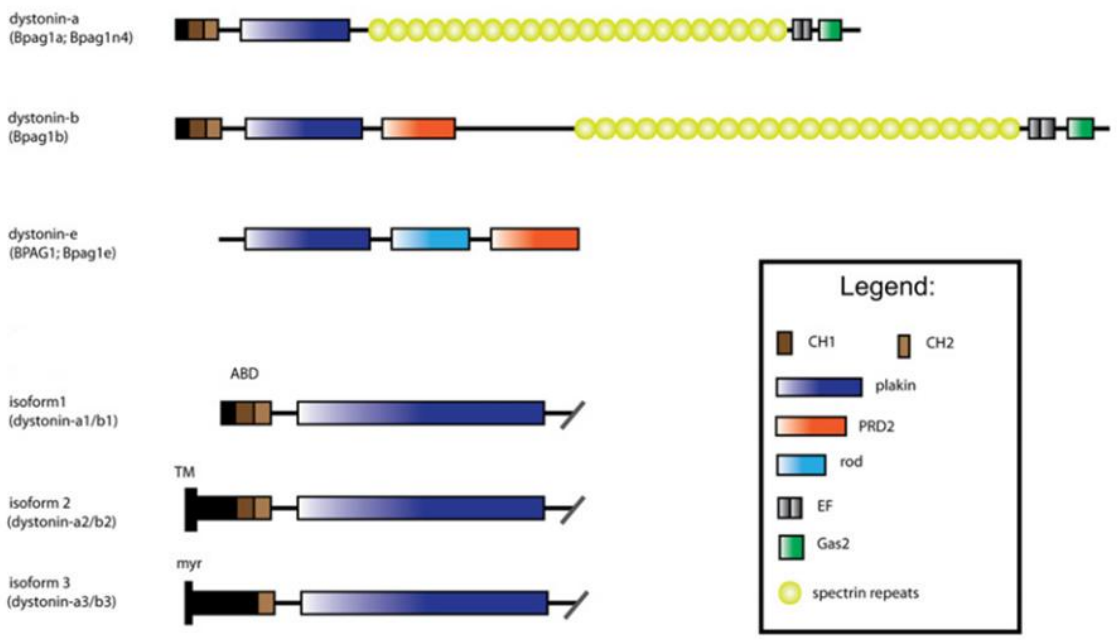

Figure 1-2: The three dystonin isoforms and the various N-terminal binding domains of dystonin-a & -b (adapted from Ferrier et al. 2013)

Figure 1-2 demonstrates that dystonin-e differs considerably from dystonin-a and dystonin-b. This epithelial isoform lacks spectrin repeats, making it similar to the non-spectraplakins described later (see section 1.4.5).

1.4.3. MACF

Microtubule-Actin Crosslinking Factor (MACF) is another important structural protein of the spectraplakin family with an N-terminal Actin binding domain and a C-terminal Growth Arrest Specific 2 (GAS2)-like protein domain which binds to microtubules (Sun et al. 2000). MACF contains 23 spectrin repeats which serve to elongate the protein allowing it to span large

distances within the cell - crucial for its function. It is the most similar protein to *Drosophila* Short Stop, as is its function (Sanchez-Soriano et al. 2009). It is also similar to dystonin, sharing up to 88% sequence similarity at the amino acid level (Karakesisoglou 2000). When the function of MACF is compromised, cellular microtubules are disorganized and structurally compromised (Karakesisoglou et al. 2000). When *short stop* (MACF analog) is inhibited through RNA interference (RNAi), microtubules networks are less able to resist forces within the cell, such as those created by molecular motors during organelle transport, and they show significant lateral movement (Applewhite et al. 2010). Knockdown of MACF in mouse neurons resulted in microtubule networks being diffuse compared to the tighter microtubule networks in normal neurons, and a similar effect was observed in a *short* stop knockdown model (Sanchez-Soriano et al. 2009). MACF also affects wound healing by inhibiting cell migration, due to the lack of microtubule networks targeting to focal adhesions, which prevents the cells from adhering to the extracellular matrix (Wu et al. 2008). These functions are important in the growth and development of muscle. Intact microtubule networks are required for proper myocyte functioning; for example in organelle transport where the myonuclei moves from the middle of the cell to the periphery during development (Wilson & Holzbaur 2012). MACF, in being the most ancestral (most related to ancestral spectraplakins) seems to also be one of the most essential plakin family members. The MACF null mouse model has been demonstrated to be embryonic lethal (Chen et al. 2006; Wu et al. 2008) and this suggests that the role of MACF in embryonic development is widespread and mandatory. This spectraplakin is highly expressed in the dermomyotome and the neural fold of 8.5 day old mouse embryos (Bernier et al. 2000), further underlining its important developmental function.

1.4.4. Plectin

Plectin is another important structural protein that is prominent in skin and muscle tissue and is the most well characterized of all the plakin family members (Wiche 1989). Plectin-null mice exhibit severe skin blistering of the limbs and, after nursing, blistering in the mouth, which is linked to inhibition of food intake and death shortly after birth (Andra et al. 1997; Ackerl et al. 2007). Plectin has binding activity with many elements of the cell which allow it to bolster the structural integrity of the cell such as Z-lines in muscle and various intermediate filaments (Wiche et al. 1984; Schröder et al. 1999; Hijikata et al. 1999). Without this reinforcement, the structural integrity of tissues is greatly compromised. Plectin contains a plakin repeat domain which, as mentioned in section 1.4.1, is comprised of modified spectrin repeats. Due to the absence of spectrin repeats (as plakin repeats are not strictly considered spectrin repeats), plectin is not classified a spectraplakin. Of the plakin family members, plectin is the only non-spectraplakin which contains an actin binding region in some variants of the protein which is composed of a calponin homology (CH) domain similar to that of other plakins (Fuchs et al. 1999; Rezniczek et al. 2003). In skin, some plectin isoforms have been found to interact with microtubules, destabilizing them (Valencia et al. 2013). As with other plakins, such as dystonin and plectin, transcript diversity is very high. There are 18 known plectin variants created through alternative splicing of 13 exons at the 5’ end, with almost no transcript diversity elsewhere in the gene (Fuchs et al. 1999). Plectins can be separated into three major classes based on their 5’ regions: mRNAs where there is one start codon compatible with the plectin reading frame, mRNAs where there are multiple upstream start codons, but translation begins at the first start codon compatible with the plectin reading frame, and mRNAs where the

first exon is non-coding and translation is not initiated at the first compatible start codon in exon 4, but instead begins in exon 6 (Rezniczek et al. 2003).

1.4.5. Other plakin family members

Given that the remaining plakin family members (desmoplakin, epiplakin, periplakin, envoplakin) have no actin binding activity, their binding activity is mediated partly though the plakin repeat domain, which binds to a variety of intermediate filaments (Leung & Liem 2001). For example, desmoplakin, a protein that is part of desmosomes, binds the desmosome to intermediate filaments such as keratin through its plakin repeat domain. Mutations in human desmoplakin cause a disruption in desmosome organization and keratin dysfunction which leads to a number of phenotypical abnormalities. These include hair with a "wooly" appearance, thick keratin plaques on the skin in areas of the body with high mechanical stresses (mostly hands and feet) as well as reduced structural integrity in heart muscle leading to heart failure in adolescence (Norgett et al. 2000). Because these plakin family members are not known to be expressed in skeletal muscle, details related to their expression profile and roles in other tissues will not be discussed in this current literature review.

1.5. Plakin expression in muscle

Plakins are expressed in many tissues including muscle. Skeletal muscles undergo significant mechanical stress during contraction and relaxation cycles and require a robust cytoarchitecture to maintain structural integrity. It is therefore not surprising that plakin crosslinking proteins such as dystonin, plectin and MACF are expressed in skeletal muscle (Boyer et al. 2010).

1.5.1. Dystonin

The role of dystonin can be elucidated by studying muscle tissue of mutant dystonin (or dystonin-deficient) mice. There are a wide variety of dystonin mutations, all causing similar phenotypes of varying intensity. Examples of these mutations are dt^{Tg4}, dt^{24J}, dt^{27J}, dt^{Alb}, , dt^{Frk}, dt^{tm1Efu} (Ferrier et al. 2013). In these mice, Z-line organization is affected. The dysfunction that follows dystonin mutations implies that dystonin interacts with Z-lines, either directly or indirectly, to stabilize them in muscle (Dalpé et al. 1999). At the cellular level, dystonin deficiency is characterized by a decreased amount of myofibrils with disorganized arrangement at the Z-disk (Dalpé et al. 1999). In addition, mitochondria, normally dispersed throughout the muscle, are found in clusters near the sarcolemma in dystonin-deficient muscle, indicating functional binding with mitochondria (Dalpé et al. 1999). These structural deficiencies are manifested at the macroscopic level through dysfunctional muscle. The muscles of dystonin-deficient mice show increased weakness, decreased fatigue resistance and are prone to contraction-induced damage (Dalpé et al. 1999). In general, dystonin is an important regulator of muscle cytoarchitecture and disruptions in dystonin cause severe muscle pathologies.

1.5.2. MACF

The role of MACF in development has already been outlined in section 1.4.3. In relation to muscle development in particular, a mutation of the *short stop* gene in *Drosophila* was shown to cause a disorganization of myotubes in muscle (Strumpf & Volk 1998). This was observed during *Drosophila* development where MHC staining to visualize myotubes showed severe disruption in the arrangement of muscle in mutant embyros relative to wild type embryos (Strumpf & Volk 1998). In mice, MACF has been shown to be strongly expressed in muscle tissue of 13.5 day old embryos (Bernier et al. 2000). Given the similarity between MACF

and Short Stop, it is possible that MACF knockout mice would also display a similar muscle phenotype as reported in *Drosophila*. However, it would be necessary to generate a MACF knockout model that would permit the animals to survive past embryonic development to be in a position to investigate the impact of MACF suppression on postnatal muscle growth. Engineering MACF muscle-specific knockdown in mice would provide a useful model to study the potential functions of MACF in skeletal muscle during post-natal development. To our knowledge, conditional knockouts have been developed in neural tissue (Goryunov et al. 2010) and skin (Wu et al. 2008) but not in muscle.

1.5.3. Plectin

As previously mentioned, plectin contains numerous isoforms. The four isoforms which are most abundant in muscle are plectin 1, 1b, 1d and 1f (Castañón et al. 2013), with P1d being the only plectin variant exclusive to muscle (Fuchs et al. 1999).

The following figure from (Castañón et al. 2013) provides an excellent summary of the various plectin variants in muscle and their function:

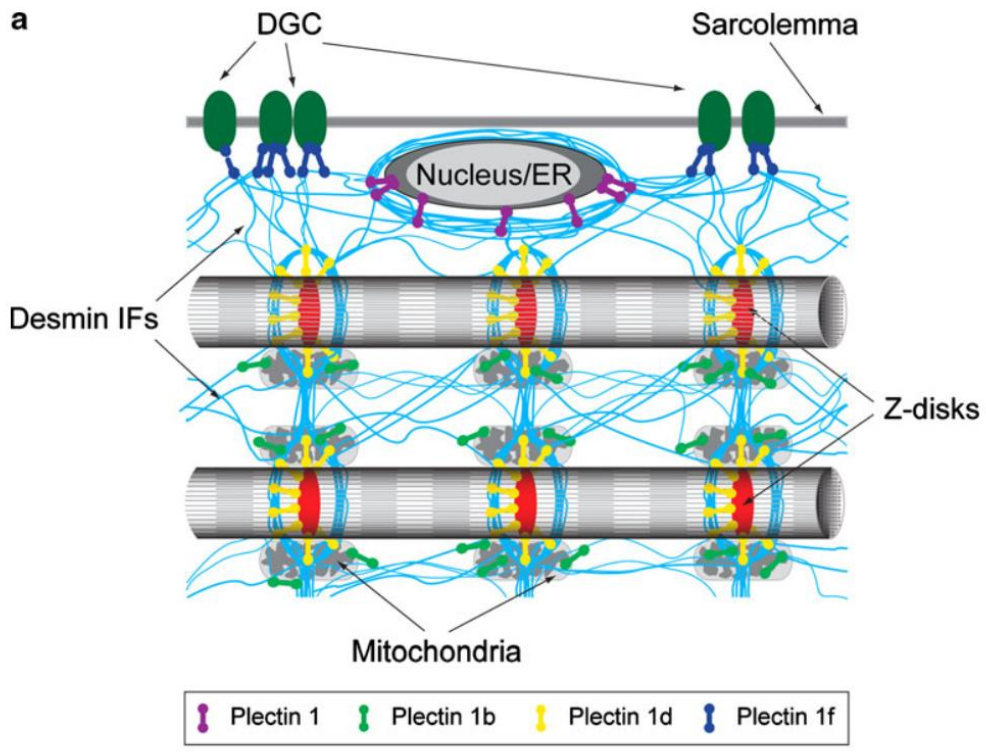

Figure 1-3: Graphical representation of the function of the four plectin isoforms present in muscle. Plectin 1 binds to the nucleus and to desmin. Plectin 1b links mitochondria to the desmin IF network. Plectin 1d crosslinks the Z-disk to the desmin IF network. Plectin 1f binds the dystroglycan complex to the desmin IF network. All these functions are crucial to the structural resilience in muscle required to resist the mechanical stresses present in contraction/relaxation cycles (taken from Castañón et al. 2013).

Desmin is the most abundant intermediate filament found in skeletal muscle (Capetanaki et al. 2007) and all plectin isoforms in muscle bind to it at their C-terminal intermediate filament binding domain. These interactions provide the extensive structural support required for the mechanical function of muscle tissue. Conditional knockout of plectin in muscle disrupts the desmin intermediate filament (IF) network (Konieczny et al. 2008). The interaction of plectin isoforms with the desmin cytoskeleton is described below.

Plectin 1 binds the nucleus and the endoplasmic reticulum to the desmin IF network, as it was found concentrated near these structures in mouse quadriceps muscle and was very diffuse in other areas of the cell (Rezniczek et al. 2007). As such, plectin 1 is thought to contribute to cellular integrity. It has been known for some time that plectin links desmin and mitochondria (Reipert et al. 1999). More recently, it was found that plectin 1b specifically is the link between mitochondria and the desmin IF network. P1b inserts itself into the mitochondrial membrane deeply enough that it resists degradation by protease enzymes (Winter et al. 2008). P1b knockout mice exhibit none of the extreme effects of total plectin deficiency and appear identical to wild type mice externally. The only apparent effect is that the shape of mitochondria in the cells of these mice becomes elongated. This can be reversed with forced expression of P1b (Winter et al. 2008).

P1d is the only plectin variant that is exclusively expressed in muscle (Fuchs et al. 1999). This is not surprising given it is only found in association with Z-disks (Rezniczek et al. 2007), which are structures unique to muscle. However, the mechanism by which P1d is targeted to Z-disks has not yet been solved (Castañón et al. 2013). P1d along with P1f seem to be the most important for the structural integrity of muscle. P1d knockout mice, as well as P1f knockout mice, have a similarly severe phenotype to that of mice lacking all isoforms (Konieczny et al., 2008, as cited in Castañón et al., 2013). This phenotype is characterized by decreased endurance, muscle with a pale appearance, aggregation of intermediate filaments, and Z-disk aggregation (i.e. forming clusters) (Konieczny et al. 2008).

Plectin 1f links the sarcolemma to the desmin IF network through the dystrophin glycoprotein complex; specifically, P1f binds to β-dystroglycan through its plakin domain, and to dystrophin via its actin binding domain (Rezniczek et al. 2007). When dystrophin is absent, plectin can also bind to β-dystroglycan with its actin binding domain, using a binding site normally occupied by dystrophin. This increases the amount of plectin localized at the sarcolemma in dystrophin-deficient mice (Rezniczek et al. 2007), a finding that is in line with previous results in muscle of Duchenne Muscular Dystrophy patients showing increased sarcolemmal plectin localization (Schroder et al. 1997). Plectin 1f also crosslinks desmin to acetylcholine receptors (AChR) at the neuromuscular junction (NMJ) at the sarcolemma (Mihailovska et al. 2014). Plectin knockout in immortalized myocytes was shown to cause AChR clusters to become more dispersed and disconnected from the desmin network (Mihailovska et al. 2014).

The structural properties of plectin can affect muscle physiology. For example, P1f has been shown to be overexpressed and to accumulate near the sarcolemma in muscular dystrophy patients and in a mouse model of muscular dystrophy, known as *mdx* (Rezniczek et al. 2007). When plectin is knocked out in *mdx* mice, the sarcolemma is no longer compromised (Raith et al. 2013). Further, while glucose uptake in muscle is impaired in *mdx* mice due to the accumulation of plectin 1f near the sarcolemma, plectin deficiency in *mdx* mice alleviates the glucose uptake impairment (Raith et al. 2013). It is therefore apparent that there is an optimal expression level and positioning of plectin and other structural proteins such as dystrophin to finely tune various aspects of muscle function.

1.6. Nerve activity and its effect on muscle physiology

The phenotype of skeletal muscle is highly regulated by signals from the innervating motor neuron. More specifically, the contractile properties of muscle fibers and their size are controlled by nerve-mediated activity and by neurotrophic molecules. Innervation also has a profound impact on gene expression in muscle cells, which governs the phenotype of skeletal muscle fibres (MacIntosh et al. 2006). In the absence of nerve activity, the expression of 205 genes is known to be differentially regulated in muscle (Magnusson et al. 2005). For instance, members of the myogenic regulatory factors, such as myogenin and MyoD, are significantly upregulated in inactivated muscles and the fact that manual electrical stimulation lessens this effect is further proof that neural activity itself is an important regulator of myogenin and MyoD gene expression (Eftimie et al. 1991).

Some of the genes whose expression are affected by reduced neural input contribute to processes underlying muscle atrophy (Kandarian & Jackman 2006). Muscle atrophy is a significant muscle condition associated with increased catabolic activity and decreased anabolic activity, with a net breakdown of protein resulting in a loss of muscle mass and force (Kandarian & Jackman 2006). Muscle atrophy in humans can be caused by inactivity, disease or aging (Kandarian & Jackman 2006). Many diseases can cause muscle atrophy including sepsis, renal failure, cancer (Hasselgren & Fischer 2001) and Amyotrophic Lateral Sclerosis (ALS) (Léger et al. 2006).

Muscle atrophy is the result of complex molecular processes involving many proteins (Powers et al. 2012; Glass 2005; Kandarian & Jackman 2006). In various experimental models of atrophy involving animals, a large number of genes are differentially regulated. However, the

gene profile is not consistent across different animals and atrophy methods (Bodine et al. 2001). Examples of genes shown to be upregulated include Muscle Ring Finger 1 (MuRF1) and Heat Shock Protein 36 (HSP36) and some examples of downregulated proteins are lactate dehydrogenase and creatine kinase (Bodine et al. 2001). Heat Shock Protein 72 was also found to be downregulated in unloaded and denervated muscle (Oishi et al. 2001). In another study, Histone Deacetylase 4 (HDAC4) was found to be responsible for gene expression changes leading to atrophy in a muscle inactivity model (Cohen et al. 2007). Upon loss of neural activity, HDAC4, normally located near synapses, relocates to the nucleus and is significantly upregulated, which leads to the changes in expression of many genes such nicotininc acetylcholine receptors (nAChRs) and myogenin. Blocking HDAC4 expression reduces this effect, implying that HDAC4 is involved in this dysregulation (Cohen et al. 2007).

1.6.1. Models of Muscle Atrophy

Muscle atrophy can be induced experimentally in animal models through reduced neural input. Some researchers use hindlimb suspension (Thomason & Booth 1990; Lawler et al. 2003). This experimental procedure utilizes a harness which elevates the hindlimb of the rats in a cage while still allowing them to move freely with the use of their forelimbs. This can be maintained for various periods of time and this type of muscle unloading causes muscle atrophy (Powers et al. 2014). In other studies, a plaster cast may be placed on the animal's limb to restrict movement (Booth & Kelso 1973; Kelleher et al. 2013). This causes atrophy in a similar fashion to hindlimb suspension. Muscle denervation is another, more severe model of muscle atrophy which will be discussed below.

Muscle denervation is the suppression of neural impulses to the muscle by severing the nerve. This procedure is well described in the literature – the animals (often mice or rats) are first anesthetised and then the sciatic nerve is severed high in the thigh, as close as possible to the sciatic notch (Dow et al. 2004; Carlson & Faulkner 1988). The nerve may be simply cut, or a small (5-10mm) portion may be removed entirely (Dow et al. 2004; Carlson & Faulkner 1988). The denervation period for various studies can vary greatly – long term studies may wish to study denervation after 12 months (Adams et al. 1995) and short-term studies may examine denervation periods of as little as one day, with periods in between ranging from 1-3 months (Batt et al. 2006) or even 1-7 days (Boudreau-Larivière et al. 2000).

Control measures are an important consideration in denervation studies. A non-denervated rat may not be an appropriate control if the animal has not been exposed to physical stress such as anaesthesia and surgery. The control protocol for denervation, referred to as "sham", is to anesthetise the animal and perform the surgery in an identical fashion to the denervated animals, stopping short of severing the nerve. In other words, the nerve is exposed but not severed (Yoshimura et al. 1999). This provides a control that is more appropriate for comparison.

1.6.2. Effects of denervation

Denervation leads to atrophy of muscle that is manifested by a reduction in cross-sectional area of muscle fibers, a loss of muscle mass, and also a significant (almost total) loss of muscle force, after a sufficient period of time. After only two months of denervation, rat muscles can lose 69% of original mass and 98% of original force (Carlson & Billington 1996). After 22 months, muscles are atrophied to the point where their thickness is similar to that of

their tendons (Carlson & Faulkner 1988). This clearly underlines the importance of nerve-mediated muscle activity to maintain the health of the muscle tissue.

Denervation seems to revert the muscle to an embryonic expression profile. For instance, during embryonic fetal development, before myocytes are innervated, nicotinic acetylcholine receptors are expressed throughout the muscle fiber. They are then repressed everywhere except the neuromuscular junction in mature myocytes (Sanes & Lichtman 2001) after the developing muscle in the fetus has been innervated. The nicotinic acetylcholine receptors (nAChR) expressed in embryonic myocytes are composed of different subunits than in mature myocytes, and denervation causes the expression of embryonic-type receptor subunits until about 1-2 months, where the mature receptor subunits begin to be expressed again (Adams et al. 1995). In this case, it seems that denervation causes the muscle to express proteins that are normally exclusively expressed in the developing embryo, for a limited amount of time. The myogenic transcription factor myogenin, which is highly expressed during myotube differentiation, is virtually undetectable in the muscles of post-natal animals (Eftimie et al. 1991). However in denervated muscles, myogenin expression is significantly upregulated (Hyatt et al. 2003; Eftimie et al. 1991) for a similar period of time as nAChR further highlighting the reversion of muscle to an embryonic state upon denervation (Adams et al. 1995)

A variety of proteins are differentially expressed in muscle following denervation (Tang et al. 2000). These include calpain-3, TNF Type 1 receptor associated protein (TRAP-2), Pre-B cell enhancing factor (PBEF), Muscle specific enolase (MSE), Myosin heavy chain IIb (MHCIIb) as well as Glutamine synthetase (GS) (Tang et al. 2000). Denervation was also shown to have an

effect on the expression of various structural elements in muscle. For example, desmin, an abundant intermediate filament which was discussed above, was shown to be upregulated in denervated rat facial muscle after two weeks, although after seven weeks expression levels of desmin returned to normal (Tews et al. 1997). Desmin was also shown to be upregulated in denervated rat gastrocnemius muscle as was tubulin (Boudriau et al. 1996). The large structural protein titin was differentially regulated in denervated skeletal muscle (Chen et al. 2005). It was shown to be downregulated by 4% starting at 7 days post denervation with a 25% reduction observed after 56 days of denervation. In contrast, dystrophin as well as β-dystroglycan, components of the dystroglycan complex discussed earlier, are upregulated following denervation. This upregulation coincides with the increased expression and reappearance of acetylcholine receptors within extra-synaptic regions of the sarcolemma following denervation (Biral et al. 1996). How denervation impacts the expression of other structural proteins such as plakin crosslinking proteins in skeletal muscle is currently not fully understood.

1.7. Statement of the problem

Plectin, dystonin and MACF are plakin crosslinking proteins that are expressed in skeletal muscle. These proteins play a critical role in organizing the cytoskeleton and crosslinking organelles and the cell membrane to intermediate filaments in various tissues, including muscle. Muscle tissue is a force generating tissue that is highly influenced by neural activity. An absence of neural activity has been shown to cause dysregulation of many genes within the muscle. *The expression patterns of plectin, dystonin and MACF in muscle during denervation-induced atrophy is poorly understood.* Specifically, it is not known whether these muscle plakins are differentially expressed at the protein or mRNA level in this model, and if

they are, whether they are downregulated or upregulated. As a whole, the findings of the present research are anticipated to further our understanding of the impact of innervation on muscle plakin expression in skeletal muscle.

1.8. Hypotheses

The three hypotheses tested were:

1) MACF will be upregulated in denervated muscle at the mRNA and protein level.
2) Dystonin will be downregulated in denervated muscle at the mRNA and protein level.
3) Plectin will be downregulated in denervated muscle at the mRNA and protein level.

Chapter 2

2. Materials and Methods

2.1. Mouse information and denervation procedure

Two-month old male CD1 mice were purchased from Charles River Laboratories (Saint-Constant, Québec) and were kept in plastic shoebox cages in groups of 4-5 mice per cage. Mice had access to food and water *ad libitum*, and were exposed to a 12 hour light/dark cycle in a climate controlled room (23±2°C). Animals were treated in accordance with the Canadian Council on Animal Care guidelines. This study was approved by the Laurentian University Animal Care Committee (see Appendix D for approval certificate).

Mice were anesthetised using isoflurane (5% for induction 1-3% for maintenance) with a 3:1 mix of air to oxygen The skin overlying the sciatic nerve was shaven and cleaned using hibitane and iodine. Denervation was performed under aseptic conditions. Mice were denervated unilaterally by severing the sciatic nerve near the hip area. The opposite limb was sham-denervated; these limbs had their sciatic nerve exposed, but it was not severed. Mice were then sutured with sterile clips and left to recover. The denervation status was confirmed by the *absence* of the toe pinch, toe spread and plantar flexion reflexes. All three of these reflexes were evident in the sham limb (i.e. non-denervated). After 1, 3, 7 or 14 days, mice were anesthetized with a xylazine (10 mg/kg bodyweight) and ketamine HCl (100mg/kg bodyweight) mix and the gastrocnemius skeletal muscles were carefully harvested from the denervated and sham hindlimb and quickly frozen in liquid nitrogen. Muscle samples were stored at -80^{o}C until further use.

2.2. Sample preparation

Mouse gastrocnemius muscles were divided in half; one half was processed for RNA extraction and the other half for protein isolation. For RNA isolation, TRIzol (Life Technologies, Gaithersburg, MD) was used as per manufacturer's instructions. RNA pellets were resuspended in RNase-free water then frozen at −80^{o}C until further use. For protein isolation, muscle samples were homogenized in radioimmune precipitation assay (RIPA) buffer supplemented with protease inhibitors (RIPA: 150mM sodium chloride, 1.0% v/v Triton X-100, 0.5% w/v sodium deoxycholate, 0.1% w/v sodium dodecyl sulphate, 50mM Tris, pH 8.0; protease inhibitors: 2µg/ml aprotinin, 10µg/ml leupeptin, 1µg/ml Pepstatin A, 1mM PMSF, 5mM EDTA, 1mM EGTA, 10mM Sodium Fluoride, 1mM sodium orthovanadate). 300 µL of RIPA buffer was used per 25mg of tissue. To homogenize muscle, a tissue tearor (Biospec products, Bartsville, USA) was used in 15 second pulses until sample was homogenous. Samples were then incubated at 4°C for 4 hours under constant agitation and then centrifuged (12,000RPM at 4°C) for 20 minutes. The supernatant from each sample was collected and stored at -80^{o}C until further use.

RNA and protein concentration for each sample was then determined. RNA was quantified by diluting an aliquot in TE buffer and measuring the absorbency at 260/280nm wavelengths using a spectrophotometer. The 260/280 ratio was used to assess phenol/protein contamination. Our samples were deemed of sufficient quality (contaminant-free) to proceed with analysis. RNA concentration was calculated based on the conversion factor of 1 unit absorbency equaling 40µg/ml of RNA. Aliquots of the RNA samples were then run on an ethidium-bromide stained agarose gel to determine the integrity of the samples and to ensure

that no degradation had occurred during the isolation procedure (see Figure 2-1 for a representative example). RNA integrity was deemed of acceptable quality when the 28S and 18S ribosomal RNA bands were clearly evident with no observable smearing and when the 28S band was roughly twice as intense as the 18S band (see Appendix A for all RNA agarose gels).

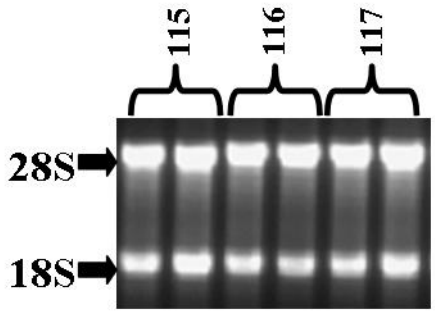

Figure 2-1: RNA integrity gel. Shown are three representative den/sham sample pairs from mice 115, 116 and 117. The clear 28S (top) and 18S (bottom) bands demonstrate that the RNA is not degraded. For additional information see Appendix A.

Protein lysate concentrations were quantified using the Bio-rad Detergent Compatible (DC) protein assay (Bio Rad, Missisauga, Canada) on a 96 well microplate using a 1:7 sample dilution. The procedure was performed according to manufacturer's instructions and read on a Biotek Powerwave-X Microplate reader at 750nm (Biotek, Ottawa, Canada). Final protein concentrations were determined from a standard curve generated from BSA samples with known concentrations processed in parallel. Regression analysis of the absorbency data was performed using the KC Junior software (Biotek, Ottawa, Canada).

2.3. Immunoblot analysis

8 protein samples from each time point (1, 3, 7 and 14 day) were separated on each gel (4% stacking, pH 6.8; 4% resolving, pH 8.8). This included 4 denervated (den) samples and their 4 contralateral control (sham) muscles. In total, 8 muscles along with the corresponding 8 contralateral controls were processed for each time point. 100ug of the protein lysates were resolved on SDS/4% polyacrylamide gels (SDS-PAGE) along with a HiMark pre-stained protein ladder (Life Technologies LC5699). Samples were treated with Laemmli's Buffer (63mM Tris HCl, 10% (v/v) Glycerol, 2% (w/v) SDS, 0.0025% (w/v) bromophenol blue, pH 6.8, 5% ß-Mercaptoethanol (v/v)) and heated at 100°C for five minutes then cooled for five minutes, on ice, prior to loading. Acrylamide gels were electrophoresed for 120 minutes in SDS electrophoresis buffer (25mM Tris base, 190mM Glycine, 0.1% w/v SDS) then were transferred onto a polyvinylidene fluoride (PVDF) membrane (0.45µM pore size, Millipore corporation, Billerica, USA) in transfer buffer (25mM Tris base, 190mM Glycine, 15% v/v methanol). Membranes were then blocked for one hour in 5% w/v milk in Tween Tris-buffered Saline (TTBS) (50mM Tris, 150mM NaCl, 0.05% v/v Tween 20, pH 7.6) and then incubated with either mouse mono-clonal plectin (Santa Cruz sc-33649), polyclonal rabbit dystonin (Sigma Genosys, custom) and mouse mono-clonal MACF (Santa Cruz sc-68430) antibodies at 1:200 dilution in 5% milk in TTBS overnight at 4°C under constant agitation. Membranes were then washed in 3 separate 10 minute TTBS washes then incubated with the corresponding goat anti-mouse (Santa Cruz sc-2005) or anti-rabbit (Santa Cruz sc-2030) secondary antibodies conjugated to horseradish peroxidase at a dilution of 1:50000 in 5% milk in TTBS at room temperature for 30 minutes on a rocking platform (Model 200, VWR scientific) then washed again (3x10 minute washes in TTBS), and subsequently developed with Enhanced Chemi Luminescence (ECL)

reagents (GE healthcare RPN2232). Membranes were stripped of antibodies and re-probed after each immunoblotting experiment, and stripped a final time before staining the membrane with Coomassie brilliant blue to verify protein loading to be used as a loading control. Stripping was performed by incubating the membrane in stripping buffer (1% SDS (w/v), 0.8% ß-Mercaptoethanol (v/v) and 0.0625 Tris HCl, pH 6.8) under light agitation at 50°C for 30 minutes then thoroughly rinsing the membranes with distilled water before washing 3x15 minutes in TBS-T. The membrane was then blocked, incubated with secondary antibody and imaged with 5 minute exposures to ensure lack of signal. The membranes were imaged using the ChemidocXRS machine (Bio-rad, Missisauga, Canada). Densitometry analysis was performed using QuantityOne software (Bio-rad, Missisauga, Canada) by outlining the bands and subtracting the background intensity from the average band intensity.

2.4. Quantitative PCR Analysis

RNA was first reverse transcribed using the Qiagen QuantiTect Reverse Transcription kit, as per manufacturer's instructions. For PCR analysis, the Qiagen QuantiTect Primer Assay was used with the following primers: actin (QT00095242), plectin (QT00288589), myogenin (QT00112378), acetylcholinesterase (AChE; QT00287357), dystonin (QT01771308), tubulin (QT00116319), MACF (QT00243670), and ribosomal protein S12 (RPS12; QT00317317) as per manufacturer's instructions. AChE and myogenin were used as positive denervation controls, as marked downregulation (AChE) and upregulation (myogenin) have been shown to occur following denervation (Eftimie et al. 1991; Sketelj et al. 1998; Boudreau-Larivière et al. 2000). Actin, tubulin and RPS1 were included as potential internal control candidates, since mRNAs with stable expression following denervation are required to normalize expression levels of

target mRNAs. 8 denervated samples from each (1, 3, 7 and 14 day) time point, along with the corresponding contralateral control sample, were loaded in duplicate onto 96 well plates, incubated at 95°C for 15 minutes followed by 40 cycles of denaturation at 94°C for 15s, annealing at 55°C for 30s and extension at 72°C for 30s in a PTC-200 thermal cycler equipped with a Chromo4 Real Time PCR instrument (MJ Research). Every 96 well plate also included a standard curve created using serial dilutions, each in triplicate, of a complementary DNA (cDNA) sample of known concentration. The data was collected using the Opticon Monitor software (MJ Research) and a C(t) score standard curve equation was created to extrapolate the abundance of the target mRNA in the denervated versus the control sham samples over the denervation time course. The C(t) score ranges for all samples and standard curves are shown in Table I. PCR efficiency ranged between 75-105%. PCR data was normalized to RPS12 as it was considered to be the most reliable (i.e. stably expressed in SHAM vs DEN samples) internal control (see Figure 2-2). Quantitative PCR data was expressed as a ratio of normalized den to normalized sham samples, where a den/sham ratio greater than 1 indicates an upregulation following denervation, and a den/sham ratio less than 1 indicates downregulation following denervation.

Table I: C(t) score range for the standard curve and the experimental samples. Two plates were run for each primer tested and these are shown separately. The majority of samples were within the range of the standard curve.

	Plate 1				Plate 2			
	Std. Curve Min	Std. Curve Max	Samples Min	Samples Max	Std. Curve Min	Std. Curve Max	Samples Min	Samples Max
AChE	20.82	34.76	21.79	29.94	20.75	34.29	23.04	31.35
Actin	21.65	36.24	15.20	23.79	15.98	31.65	19.24	24.83
Dystonin	16.24	33.46	19.28	24.00	15.58	30.94	17.87	22.64
MACF	17.23	31.27	19.17	27.53	15.83	33.26	20.65	25.65
Myogenin	19.54	30.86	12.23	24.35	17.16	32.03	21.05	30.04
Plectin	15.94	35.02	18.21	23.83	15.57	32.60	18.83	23.04
RPS1	14.30	30.33	17.15	20.72	14.42	30.28	17.92	20.79
Tubulin	17.33	31.55	19.19	23.89	17.63	32.01	20.72	26.96

2.5. Data analysis

Data was analyzed in SPSS. Outliers were removed according to default SPSS settings for outliers, defined as 1.5 times the interquartile (Q3-Q1) range below the first and above the third quartile. Data was checked for normality and when the test for normality failed, the data was log-transformed and re-checked for normality. When this improved normality, log-transformed data was used for analysis. This was the case for MACF, dystonin and AChE for mRNA data and for MACF for protein data. An analysis of variance (ANOVA) was used to determine differences between den/sham pairs across the four time points for each of eight data sets (plectin, dystonin, MACF, myogenin and AChE mRNA as well as plectin, dystonin and MACF protein expression) and paired t-tests were used to assess the difference between den/sham pairs within each time point for each of the eight data sets above. The significance threshold was set at $p<0.05$.

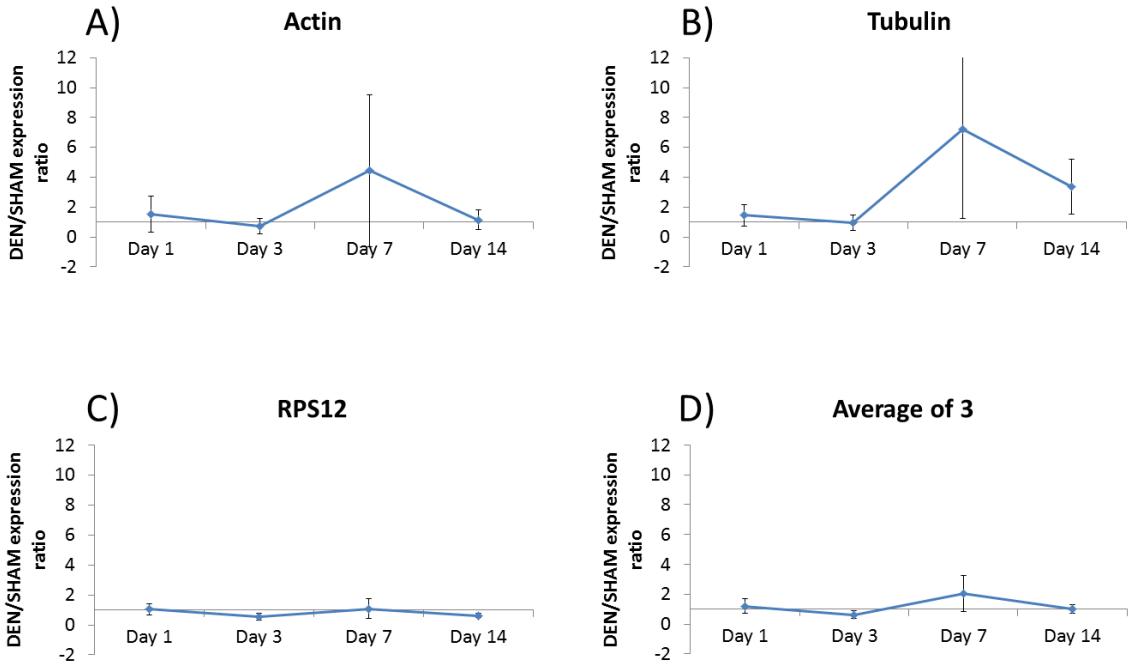

Figure 2-2: Comparison of four potential normalization candidates for qPCR data. Data are expressed as Means ± SD (n = 8 for den/sham ratio for each time point). A ratio equivalent to 1 is indicative of similar expression levels in the den and sham muscle samples. **A)** Actin den/sham ratios over the four denervation time points. Actin expression is fairly stable between the den and sham muscles at days 1, 3 and 14 but extremely variable at day 7. **B)** Tubulin expression is similar to actin, with high variability at day 7 but also increased variability at day 14. **C)** RPS12 was the most stable of all three potential normalization candidates with minimal variance. **D)** The den/sham ratios for Actin, Tubulin and RPS12 were collapsed and the means and SD were calculated. The higher variability at day 7 persisted. Based on these results, RPS12 was selected as the normalization control for the qPCR analyses because the ratios were closest to one with minimal variance.

Chapter 3

3. Results

3.1. Markers of denervation

To ascertain whether the denervation procedure was successful, the following three reflexes were monitored on a daily basis in both the sham and den hindlimb: toe spread, toe pinch and plantar flexion. In all instances these reflexes were present in the sham hindlimb and absent in the den hindlimb. Furthermore, we monitored the gastrocnemius hindlimb muscle mass as well as the gene expression levels of myogenin and AChE which are both known to be significantly upregulated and downregulated respectively in denervated skeletal muscle (Eftimie et al. 1991; Boudreau-Larivière et al. 2000; Sketelj et al. 1998).

Frozen mouse gastrocnemius muscles were weighed (in milligrams) and these values were normalized to total bodyweight of each mouse (in grams). These values are reported in Table II and displayed in Figure 3-1. As anticipated, significant muscle atrophy was observed in denervated hindlimb muscles as revealed by paired t-tests. In particular, normalized muscle mass had decreased by 6.6% after only 24 hrs of denervation ($p=0.006$), by 9.3% after 3 days of denervation ($p=0.011$), by 23.1% after 7 days ($p<0.001$) and by 41.5% after 14 days of denervation ($p<0.001$). In comparison, the left and right gastrocnemius muscles of control mice, which were anesthetized but did not undergo surgery, had nearly identical muscle mass ($p=1.000$) thereby indicating that our excision technique was consistent.

Table II. Mouse gastrocnemius mass (mg) normalized to body weight (g). Data are presented as Means ± SE (mg/g) (n = 10 for sham and den at each time point, n = 4 for control mice).

	Day 1	Day 3	Day 7	Day 14	Control
Sham	4.8±0.10	4.7±0.11	4.8±0.08	4.8±0.10	4.4±0.32
Den	4.5±0.09	4.3±0.08	3.7±0.09	2.8±0.11	4.4±0.28
% change	-6.6%	-9.3%	-23.1%	-41.5%	0.2%
p-value	0.006	0.011	<0.001	<0.001	1.000

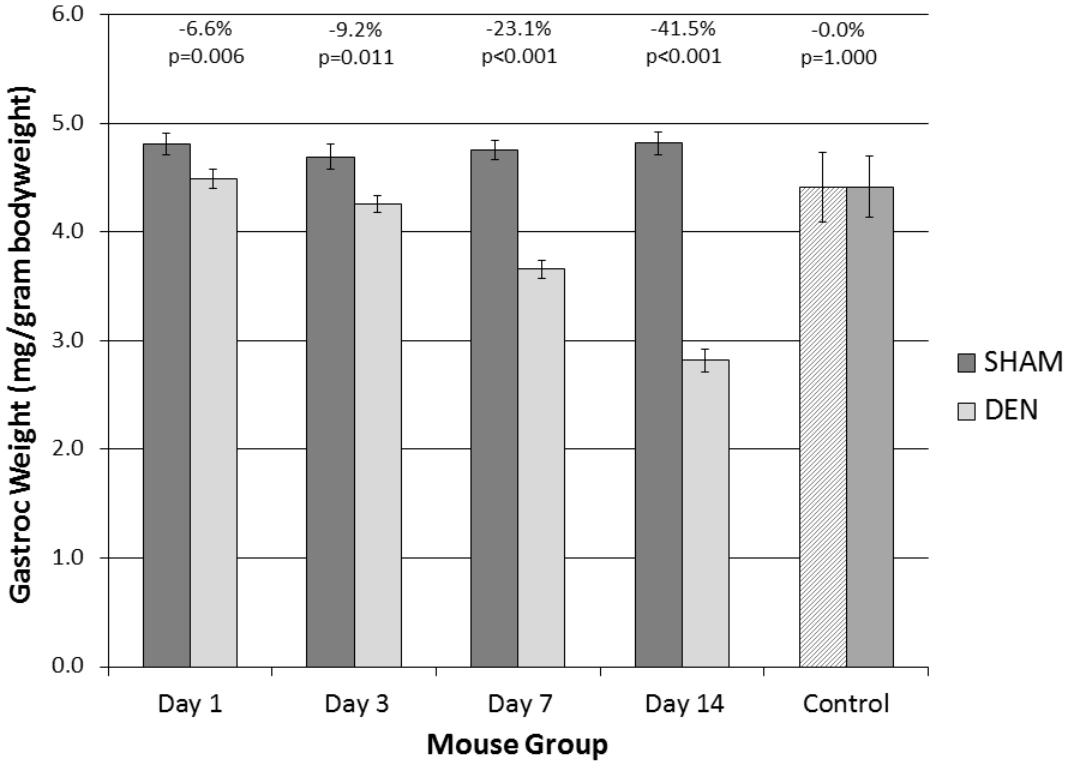

Figure 3-1: Impact of denervation on mouse Gastrocnemius muscle weight. Data are expressed as muscle weight normalized to body weight (Means ± SE). (n = 10 for sham and den mice, for each time point, n = 6 for control). Paired samples t-tests revealed statistically significant atrophy after 24 hours of denervation (7% reduction, p=0.006). Atrophy progressively worsened at every time point, leading to a 42% loss in muscle mass after two weeks of denervation (p<0.001). No significant difference was found between the right and left hindlimb muscle weights of non-denervated mice (Control).

An ANOVA was performed on the den/sham ratios for muscle weight to determine if there were statistically significant differences at the four denervation time points (Figure 3-2). The ANOVA was significant ($F_{4,45}$=17.293, p<0.000) and Tukey's post hoc tests were used to determine differences between groups. Days 7 and 14 were significantly lower than days 1, 3 as well as the control group. No other significant differences existed between groups.

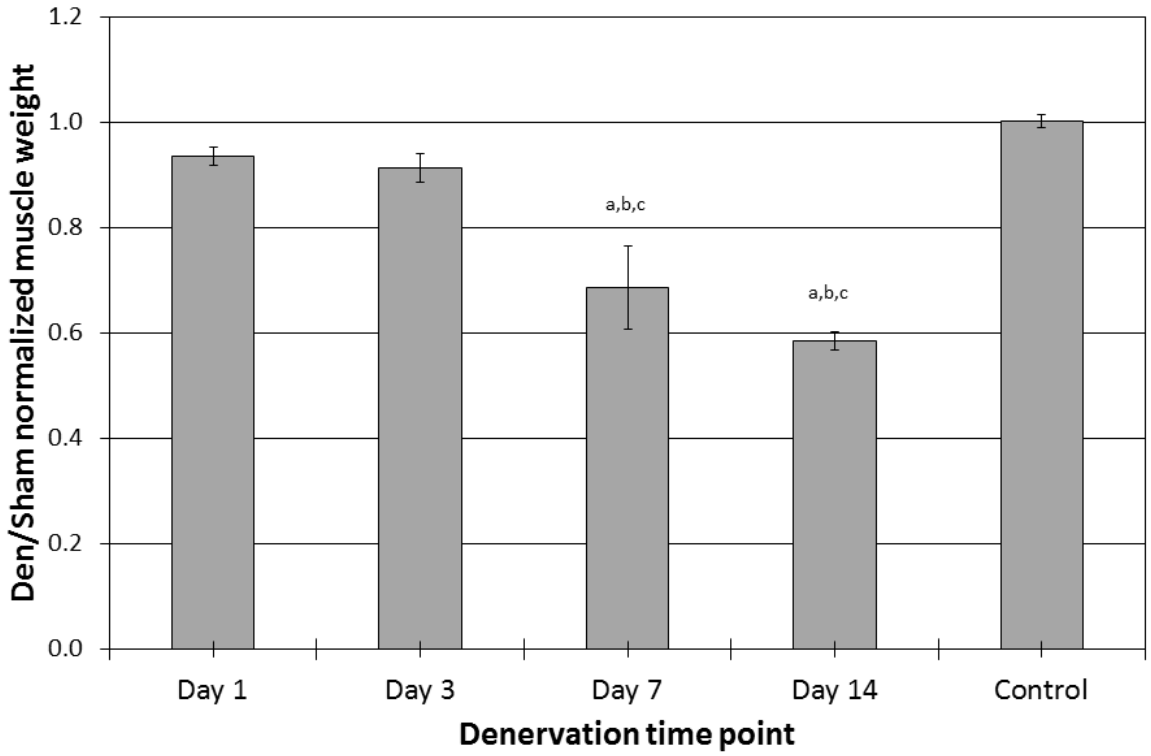

Figure 3-2: ANOVA of den/sham ratio of mouse muscle weight following 1, 3, 7 and 14 days of denervation. Data are expressed as a ratio of normalized muscle weight in den vs sham muscles (Means ± SE) (n = 10 for den/sham ratio for each time point, except for control where n=6). Days 7 and 14 were significantly lower than day 1 (a), day 3 (b) and control (c) time points. No other significant differences existed between groups.

Next, we measured the gene expression levels of myogenin and AChE in sham versus den skeletal muscle at the same four denervation time-points using qPCR. Expression levels for sham samples were set to a value of 1 for myogenin and the expression levels in the denervated samples were calculated as a ratio of den/sham. These data are presented in Table III as well as in Figure 3-3 through Figure 3-6. Paired t-tests were performed to analyze the difference between myogenin mRNA expression levels in den muscle compared to their respective contralateral sham controls. After 1 day of denervation, myogenin expression in den muscle was substantially increased by 9-fold in comparison to sham muscle ($p=0.016$). After 3, 7 and 14-days of denervation, high levels of expression for myogenin were maintained; approximately 9-fold ($p=0.001$), 12-fold ($p=0.019$) and 13-fold ($p=0.059$) respectively. An ANOVA was performed on the den/sham ratios to determine if there were statistically significant differences in myogenin expression levels at the four denervation time points (Figure 3-4). This analysis revealed that myogenin induction occurred very early in the denervation time course and was sustained over the two-week period post-denervation ($F_{3,27}=0.543$, $p=0.657$).

Table III. mRNA expression of myogenin and AChE in sham and denervated muscles after 1, 3, 7 and 14 days of denervation as assessed by qPCR. Den values were normalized to a sham value of 1. Data are Means + SE (Arbitrary unit). (n = 8 for sham and den mice for each time point). An asterisk denotes significant difference between sham and den at each time point.

	Myogenin		AChE	
	Sham	Den	Sham	Den
Day 1	1.0±0.30	9.3±2.86*	1.0±0.22	0.39±0.065*
Day 3	1.0±0.29	9.5±1.72*	1.0±0.21	0.14±0.024*
Day 7	1.0±0.21	11.6±3.53*	1.0±0.17	0.16±0.044*
Day 14	1.0±0.29	13.4±5.73*	1.0±0.29	0.12±0.056*

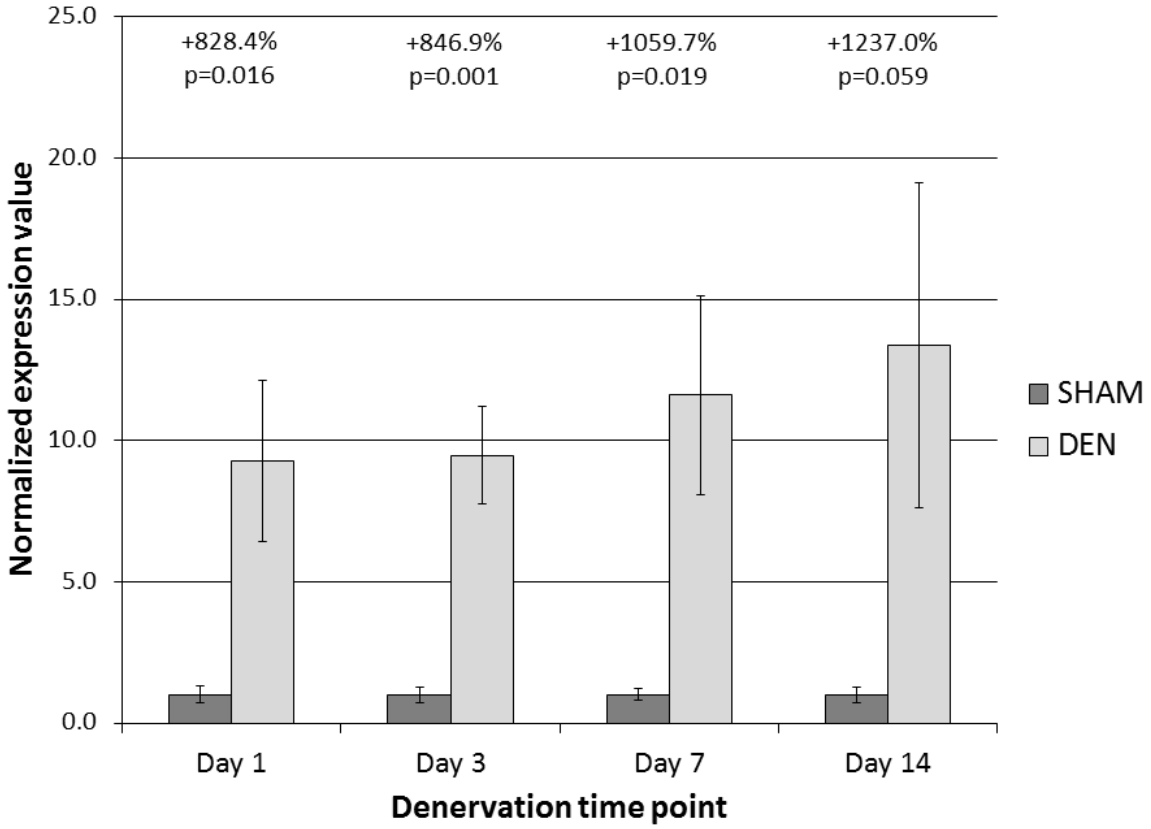

Figure 3-3: Impact of denervation on myogenin mRNA expression levels. Data are expressed as Means ± SE with den samples being normalized to a sham value of 1. (n = 8 for sham and den mice for each time point). Paired samples t-tests revealed statistically significant upregulation after 24 hours of denervation (9-fold increase, p=0.016). This increase was maintained during the following 3, 7 and 14 days of denervation, with a moderate increase in magnitude paired with higher variance at later time points.

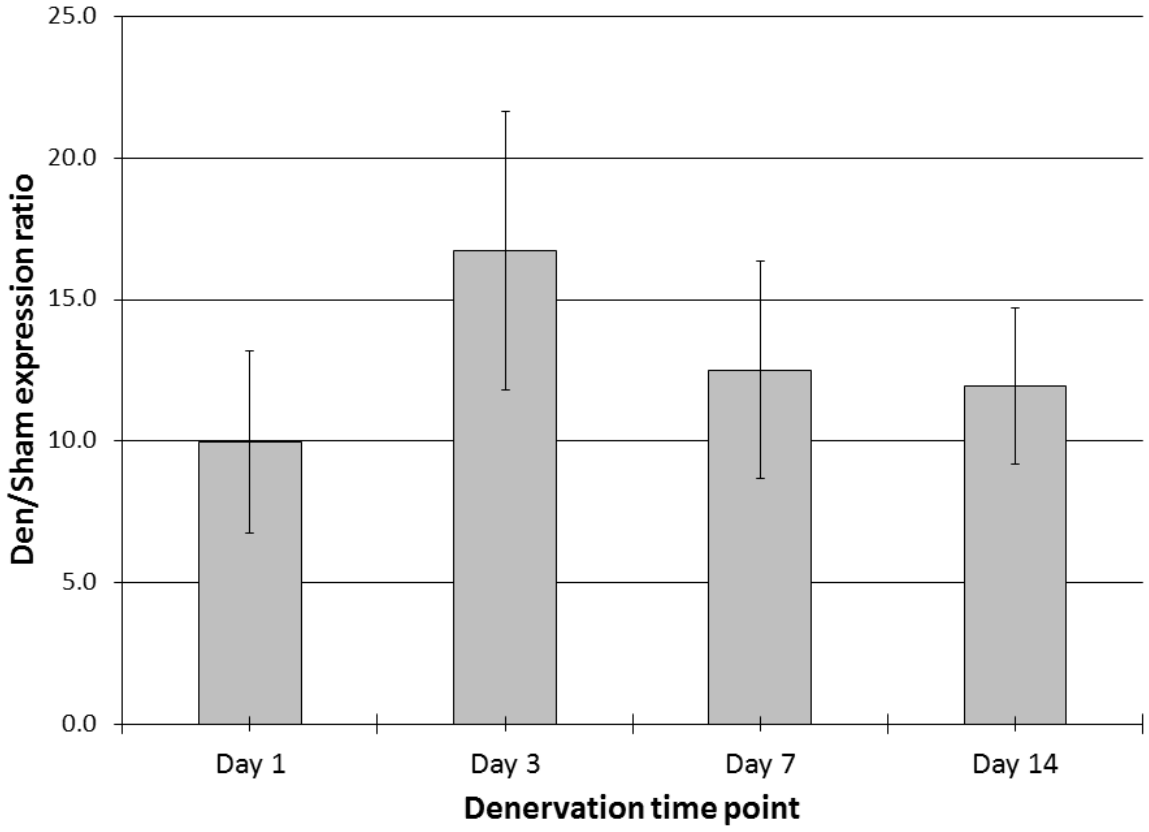

Figure 3-4: Impact of denervation on myogenin mRNA expression levels. Data are expressed as a ratio of mRNA levels in den vs sham muscles (Means ± SE) (n = 8 for den/sham ratio for each time point). After 24 hours of denervation, expression in den samples increased tenfold relative to sham samples. This upregulation is fairly stable between 1 and 14 days. ANOVA revealed no statistically significant differences in myogenin expression levels between any of these time points.

AChE expression was normalized to a sham value of 1 and these data are presented in Table III. Paired t-tests were performed to analyze the difference between AChE mRNA expression levels in denervated muscle and their contralateral sham controls. Paired t-test results are presented in Figure 3-5. One day after denervation, AChE expression in denervated muscle was reduced by 60.9% compared to sham muscle and this difference was significant with $p=0.033$. AChE expression in denervated muscle was reduced by 85.8% after 3 days ($p=0.003$) then remained fairly stable with an 84.4% reduction at day 7 and an 87.6% decline at day 14 ($p<0.001$ and $p=0.011$, respectively). An ANOVA was performed on the den/sham ratios to determine if statistically significant differences existed between AChE expression levels at the four denervation time points (see Figure 3-6). The ANOVA was significant ($F_{3,28}=10.816$, $p<0.001$) and Tukey's post-hoc tests were performed to analyze the differences between time points. AChE expression levels at days 3, 7 and 14 were significantly decreased compared to Day 1 ($p<0.001$), but the den/sham expression ratios between days 3, 7 and 14 were not significantly different from each other.

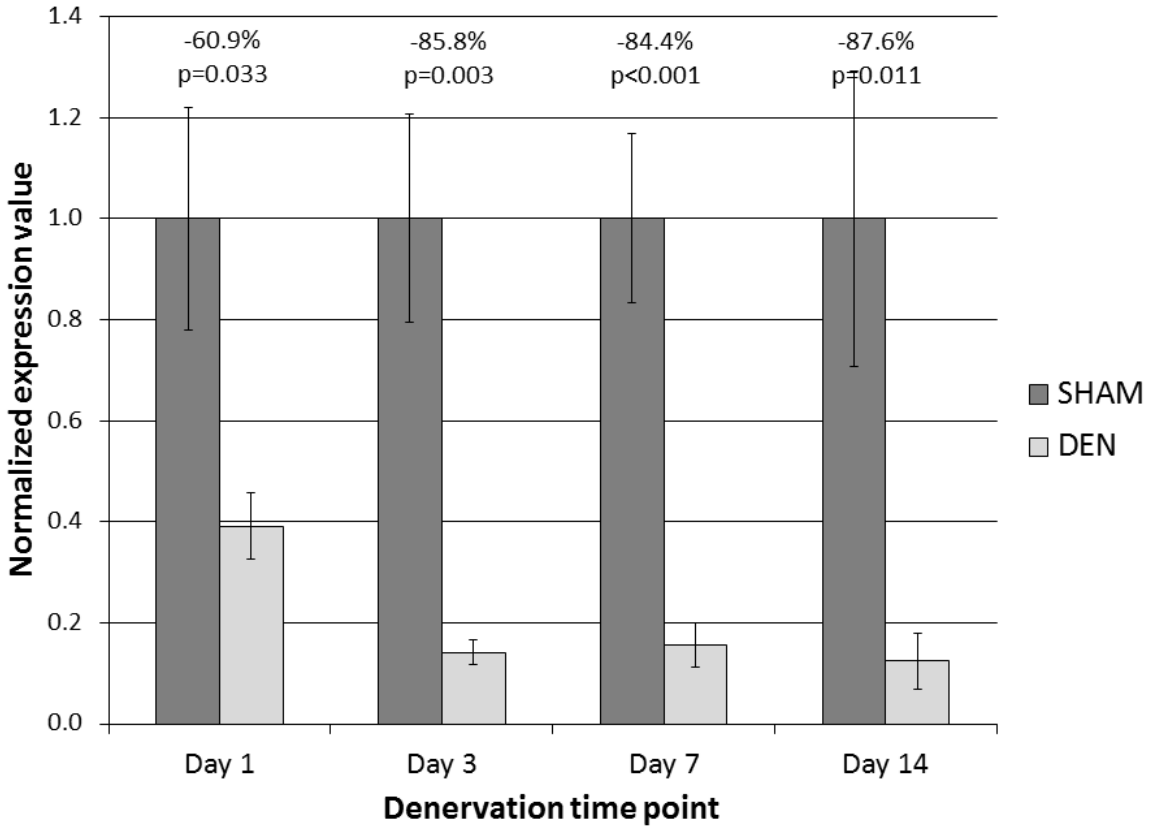

Figure 3-5: Impact of denervation on AChE mRNA expression levels. Data are expressed as Means ± SE with den samples being normalized to a sham value of 1 (n = 8 for sham and den at each time point). Paired samples t-tests revealed statistically significant downregulation after 24 hours of denervation (61% reduction, p=0.033). AChE expression levels appear to stabilize after 3 days with a downregulation of approximately 85% in denervated muscle after 3, 7 and 14 days of denervation.

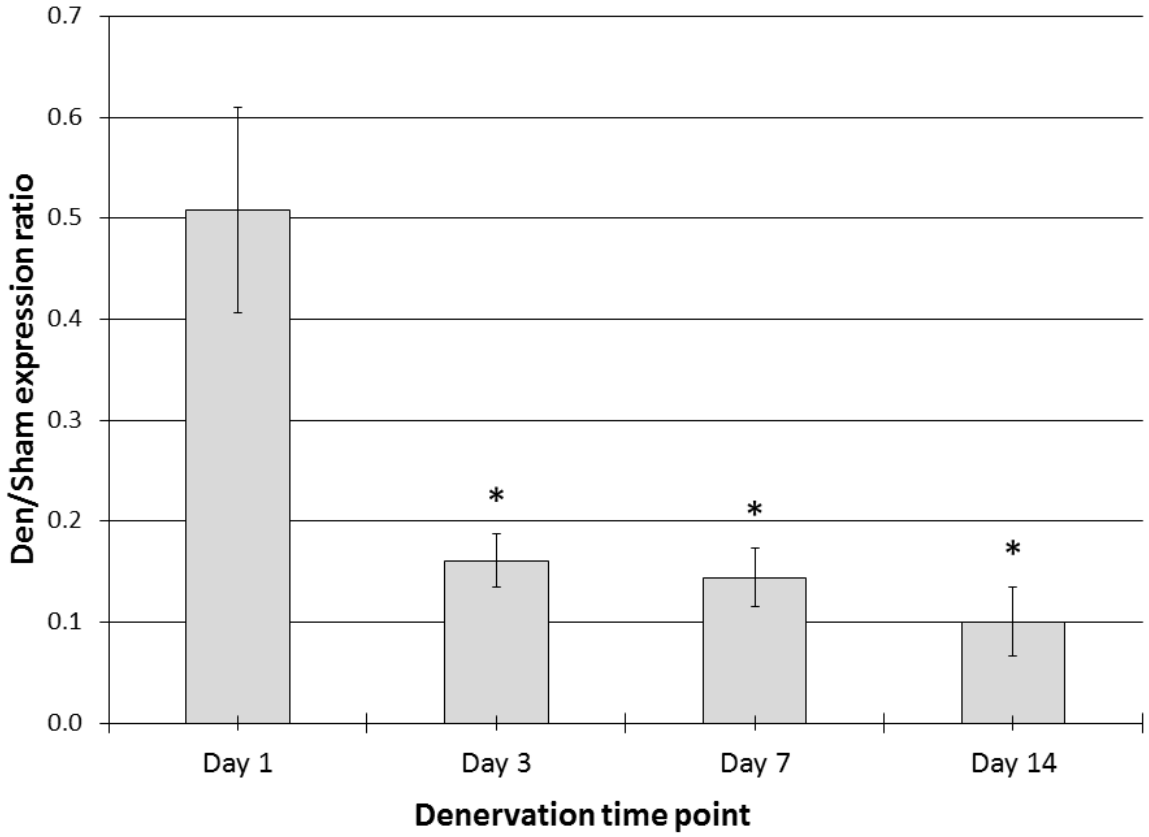

Figure 3-6: Impact of denervation on AChE mRNA expression levels. Data are expressed as a ratio of mRNA levels in den vs sham muscles (Means ± SE) (n = 8 den/sham ratio at each time point). Bars marked with an asterisk indicate values are significantly different from Day 1 expression levels. After 24 hours of denervation, expression in den samples is reduced relative to sham samples. Between days 3 and 14, expression is reduced to 10-15% in den samples relative to sham samples. These latter time points are also significantly different from day 1 expression ratios.

Collectively, the muscle weight and myogenin/AChE gene expression level data are in line with the anticipated phenotype of denervated skeletal muscle. We therefore proceeded to measure the expression profile of the three plakin family members both at the mRNA and protein levels to better understand how these cytoskeletal proteins are impacted in skeletal muscles that have been inactivated subsequent to motor neuron injury.

3.2. Gene expression of plectin, dystonin and MACF in denervated skeletal muscle

3.2.1. Plectin

Using the same cDNA samples processed for qPCR experiments to measure myogenin and AChE expression, we determined the gene expression levels of plectin. Paired t-tests were performed to analyze the difference between plectin mRNA expression levels in den muscle and their contralateral sham controls (See Table IV and Figure 3-7 for paired t-test results). Plectin mRNA levels were slightly downregulated in den muscle at day 1 (11.1% reduction) and day 3 (26.0% reduction) but these differences were not significant at the $\alpha<0.05$ significance threshold. After seven days of denervation, plectin expression was reduced by 45.7% ($p=0.019$) in den muscle and after 14 days expression was reduced by 57.5% ($p<0.001$).

An ANOVA was performed on the den/sham ratios to determine if any statistically significant differences existed between plectin mRNA expression levels at the four, denervation time points. These results are presented in Figure 3-10. The ANOVA was significant ($F_{3,28}=3.651$, $p=0.024$) and Tukey's post hoc analysis revealed that Day 14 den/sham expression ratios were significantly lower than day 1 den/sham expression ratio, but no other significant differences existed between groups.

Table IV. mRNA expression of plectin, dystonin and MACF in sham and den muscles after 1, 3, 7 and 14 days of denervation as assessed by qPCR. Den values were normalized to a sham value of 1. Data are mean + SE (n = 8 for sham and for den for each time point). An asterisk indicates significant differences from sham at that time point.

	Plectin		Dystonin		MACF	
	Sham	Den	Sham	Den	Sham	Den
Day 1	1.0±0.22	0.9±0.21	1.0±0.18	1.0±0.17	1.0±0.28	0.8±0.24
Day 3	1.0±0.21	0.7±0.18	1.0±0.21	0.7±0.16	1.0±0.27	2.1±0.53*
Day 7	1.0±0.13	0.5±0.04*	1.0±0.12	0.5±0.04*	1.0±0.14	2.6±0.40*
Day 14	1.0±0.07	0.4±0.03*	1.0±0.07	0.5±0.07*	1.0±0.09	2.1±0.43*

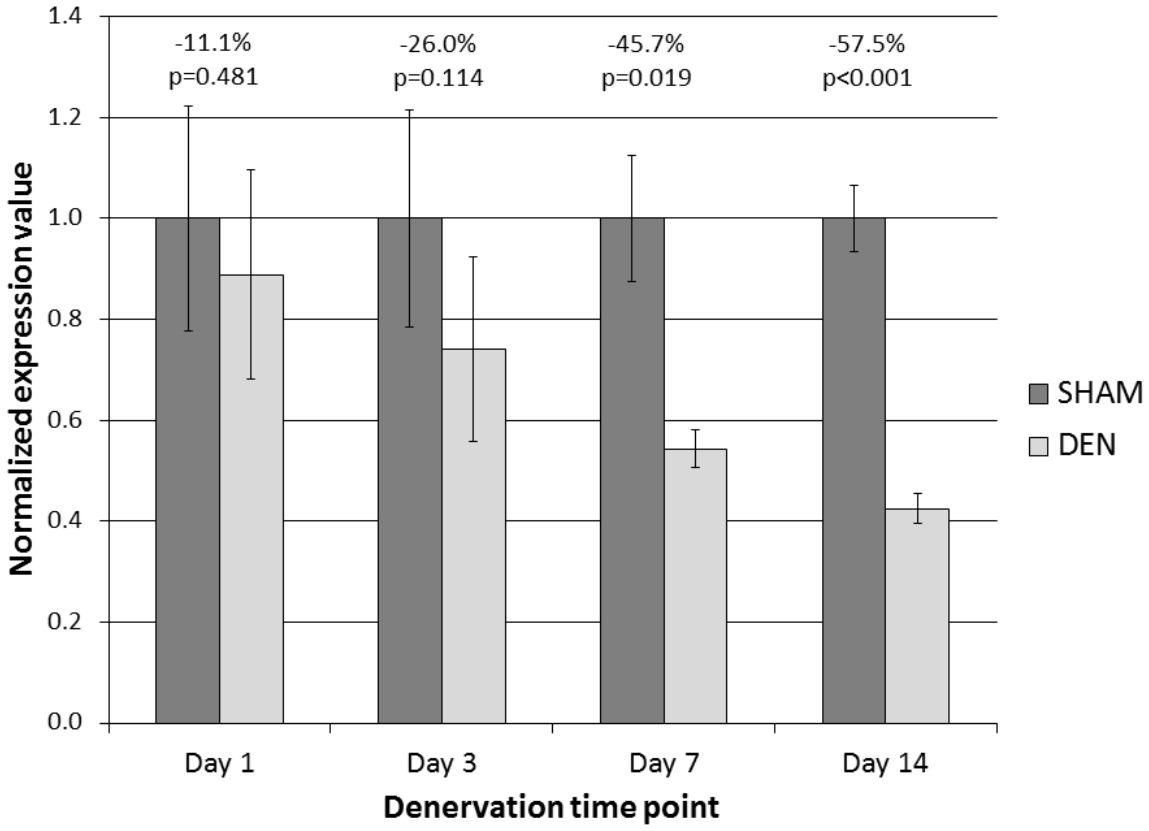

Figure 3-7: Impact of denervation on plectin mRNA expression levels. Data are expressed as mean ± SE with den samples being normalized to a sham value of 1 (n = 8 for sham and for den for each time point). Paired sample t-tests revealed statistically significant downregulation after 7 days (45.7% decrease, p=0.019) and 14 days (57.5% decrease, p<0.001) of denervation.

3.2.2. Dystonin

Paired t-tests were performed to analyze the difference between dystonin mRNA expression levels in den muscle and their contralateral sham controls (See Figure 3-8 and Table IV for paired t-test results). Dystonin mRNA expression patterns were similar to plectin, with small but non-significant reductions at day 1 (0.8% reduction, p=0.963) and day 3 (29.3% reduction, p=0.090) with more pronounced downregulation at day 7 and day 14. After seven days of denervation, dystonin expression was reduced by 45.8% in denervated muscle compared to sham controls and this difference was significant (p=0.010). After 14 days, expression was reduced by 49.4% (p<0.001).

An ANOVA was performed on the den/sham ratios to determine if any statistically significant differences existed between dystonin expression levels at the four, denervation time points and these results are presented in Figure 3-10. Again, the pattern was very similar to that of plectin. The ANOVA was significant ($F_{3,28}$=4.619, p=0.010) and Tukey's post hoc tests revealed significantly lower expression at days 7 and 14 compared to day 1 (p=0.033, p=0.009 respectively).

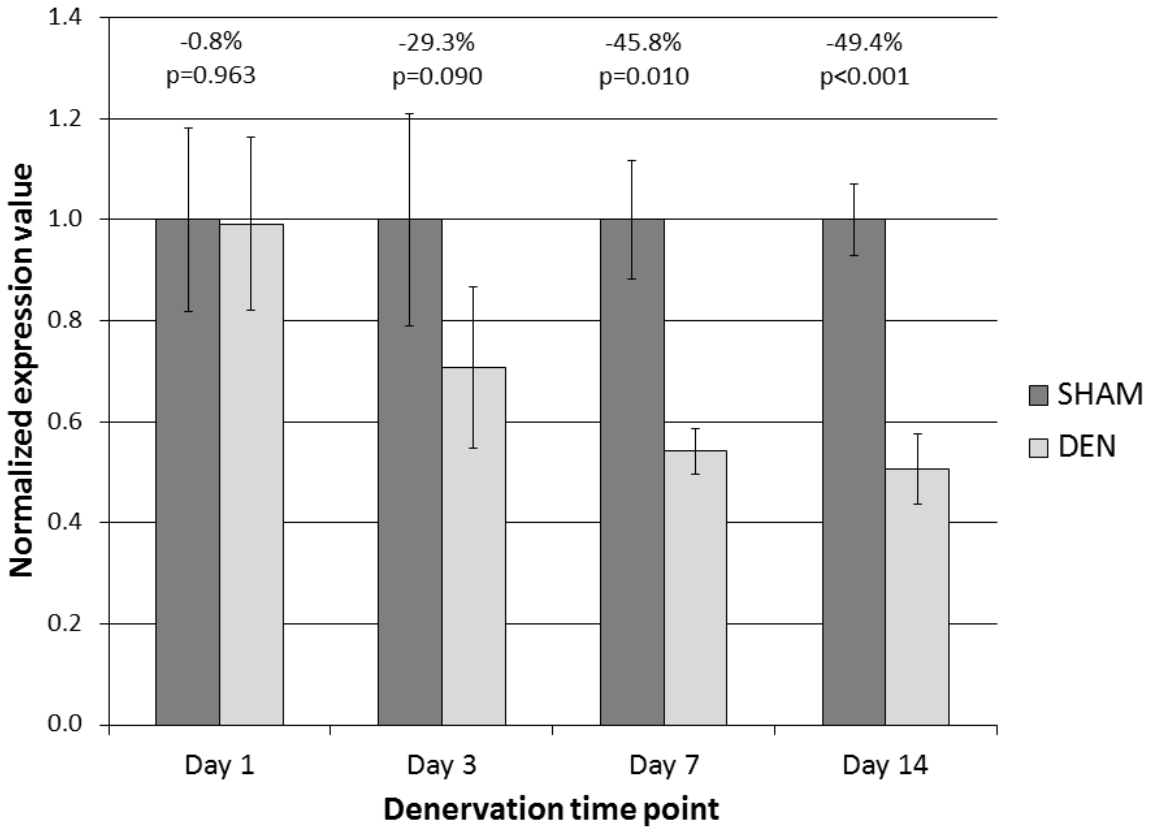

Figure 3-8: Impact of denervation on dystonin mRNA expression levels. Data are expressed as mean ± SE with den samples being normalized to a sham value of 1 (n = 8 for sham and for den for each time point). Paired sample t-tests revealed statistically significant downregulation after 7 (45.8% decrease, p=0.010) and 14 days (49.4% decrease, p<0.001) of denervation.

3.2.3. MACF

Paired t-tests were performed to analyze the difference between MACF mRNA expression levels in denervated muscle and their contralateral (sham-denervated) controls (See Figure 3-9 and Table IV for paired t-test results). MACF expression after 1 day was unaltered (p=0.494). However, after three days of denervation, expression in the den limb increased roughly twofold (112.0% increase, p=0.006). Expression then peaked after seven days of denervation with approximately a 2.5 fold (155.3%, p=0.016) increase in expression in den muscle compared to sham controls. After 14 days, expression returned to day 3 levels with a 112.9% increase (p=0.030).

An ANOVA was performed on the den/sham ratios to determine if any statistically significant differences existed between MACF expression levels at the four denervation time points. These results are presented in Figure 3-10. The ANOVA was significant ($F_{3,27}$=4.709, p=0.009) and Tukey's post hoc tests show that the Den/Sham expression ratios for MACF were significantly increased at day 3, day 7 and day 14 compared to day 1 ($p<0.05$).

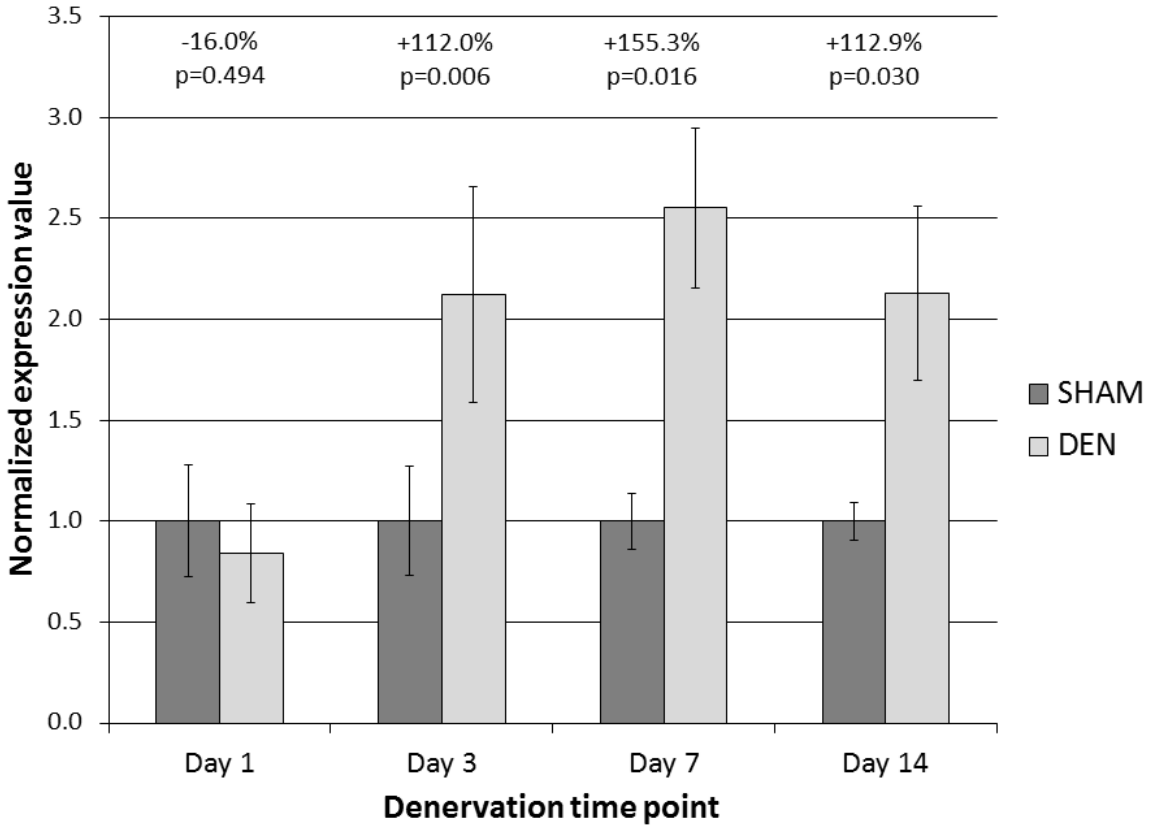

Figure 3-9: Impact of denervation on MACF mRNA expression levels. Data are expressed as mean ± SE with den samples being normalized to a sham value of 1 (n = 8 for sham and for den for each time point). Paired sample t-tests revealed statistically significant upregulation beginning at day 3 (2-fold increase, p=0.006) and persisting through day 14 (2-fold increase, p=0.030), with a peak in expression at day 7 (2.5-fold increase, p=0.016).

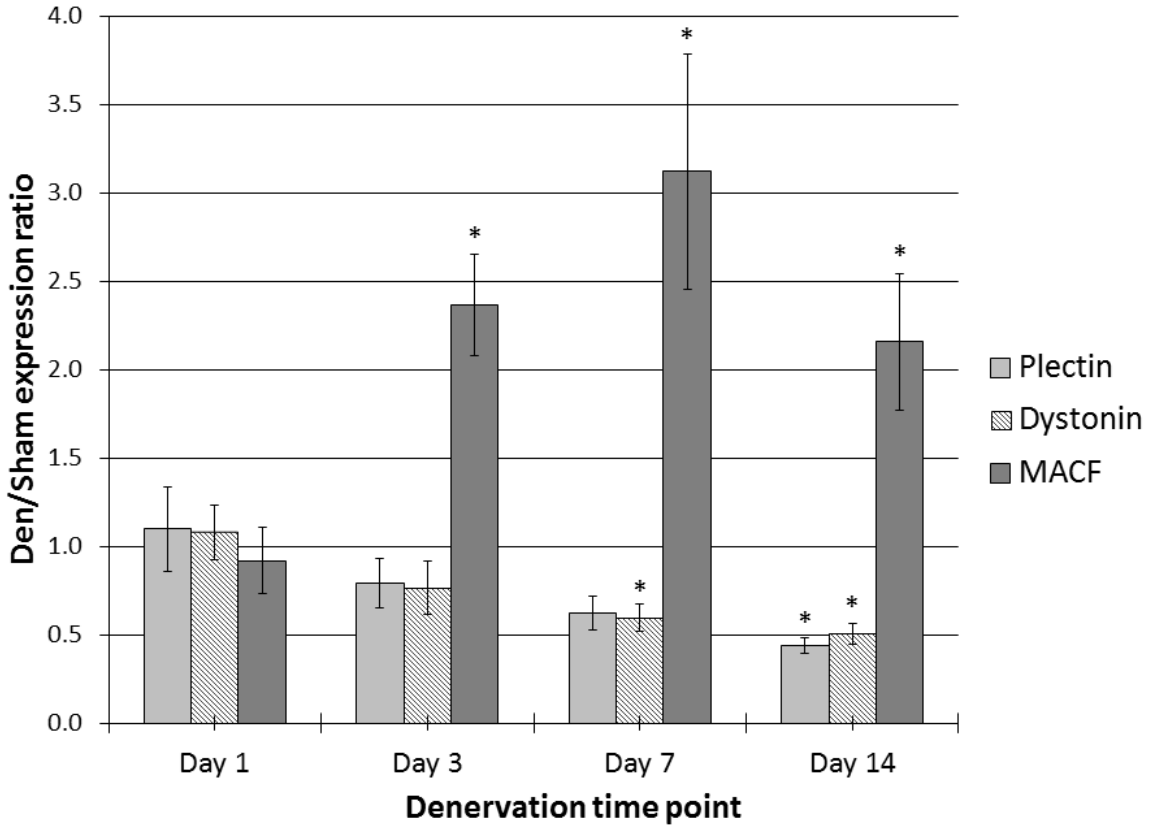

Figure 3-10: Impact of denervation on plectin, dystonin and MACF mRNA expression levels. Data are expressed as a ratio of mRNA levels in den vs sham muscles (mean ± SE) (n = 8 for den/sham ratio for each time point). Bars marked with an asterisk indicate values that are significantly different from Day 1 expression levels relative to each plakin target. Both plectin and dystonin gene expression were progressively reduced over the denervation time course. By Day 14, mRNA levels for plectin and dystonin were reduced by half compared to Day 1 levels. In contrast, MACF gene expression was significantly upregulated at Days 3, 7 and 14 relative to Day 1, with expression in den muscle peaking at roughly 3 times the expression levels in the contralateral sham limb.

3.3. Protein expression of plectin, dystonin and MACF in denervated skeletal muscle

3.3.1. Plectin

Protein levels were determined by 'high molecular weight' Western blotting. Paired t-tests were performed to analyze the difference between plectin protein expression levels in den muscle and their contralateral sham controls. The results of the Paired t-tests are depicted in Figure 3-11 as well as in Table V. Overall, the protein levels for plectin remained similar between the sham and den samples over the course of the denervation time course. An ANOVA performed on the den/sham ratios also revealed that the ratios were similar over the course of the denervation time course ($F_{3,24}$=0.640, p=0.597, see Figure 3-12).

3.3.2. Dystonin

Paired t-tests were performed to analyze the difference between dystonin protein expression levels in den muscle and their contralateral sham controls (see Figure 3-11 and Table V for results). Dystonin expression was unchanged after one day and three days of denervation (p=0.857, p=0.077 respectively). In comparison, dystonin was significantly upregulated after seven days (50.2% increase, p=0.019) and fourteen days of denervation (30.5% increase, p=0.005).

An ANOVA was performed on the den/sham ratios and the results are summarized in Figure 3-12 and Table V. The ANOVA was significant ($F_{3,28}$=5.083, p=0.006) and Tukey's post hoc tests revealed that den/sham expression ratios for dystonin at days 7 and 14 were significantly increased from day 1 (p=0.014 and p=0.017, respectively). No other significant differences were found between time points.

3.3.3. MACF

Paired t-tests were performed to analyze the difference between MACF protein expression levels in den muscle and their contralateral sham controls (see Figure 3-11). MACF expression was unchanged at day 1 ($p=0.774$) and at day 3 post denervation ($p=0.059$). After seven days, expression was transiently upregulated (67.4% increase, $p=0.002$) but returned to sham levels by day 14 ($p=0.246$).

Results from an ANOVA performed on the den/sham ratios are summarized in Figure 3-12. The ANOVA was significant ($F_{3,28}=4.663$, $p=0.009$). Tukey's post hoc tests revealed that MACF expression at day 7 was significantly upregulated compared to days 1, 3 and 14 ($p<0.05$); no other significant differences were found between time points.

Table V. Plectin, dystonin and MACF protein expression in sham and den muscles after 1, 3, 7 and 14 days of denervation as assessed by densitometry. Den values were normalized to a sham value of 1. Data are expressed as the mean +/- SE (n = 8 for sham and for den for each time point, except plectin day 1 where n=6 due to removal of outliers). An asterisk indicates significant differences between sham at that time point.

	Plectin		Dystonin		MACF	
	Sham	Den	Sham	Den	Sham	Den
Day 1	1.0±0.44	0.9±0.22	1.0±0.27	0.9±0.25	1.0±0.08	0.9±0.15
Day 3	1.0±0.13	1.2±0.20	1.0±0.04	1.2±0.04	1.0±0.21	1.1±0.20
Day 7	1.0±0.26	1.6±0.39	1.0±0.25	1.5±0.42*	1.0±0.29	1.7±0.22*
Day 14	1.0±0.24	1.2±0.31	1.0±0.04	1.3±0.06*	1.0±0.16	1.1±0.18

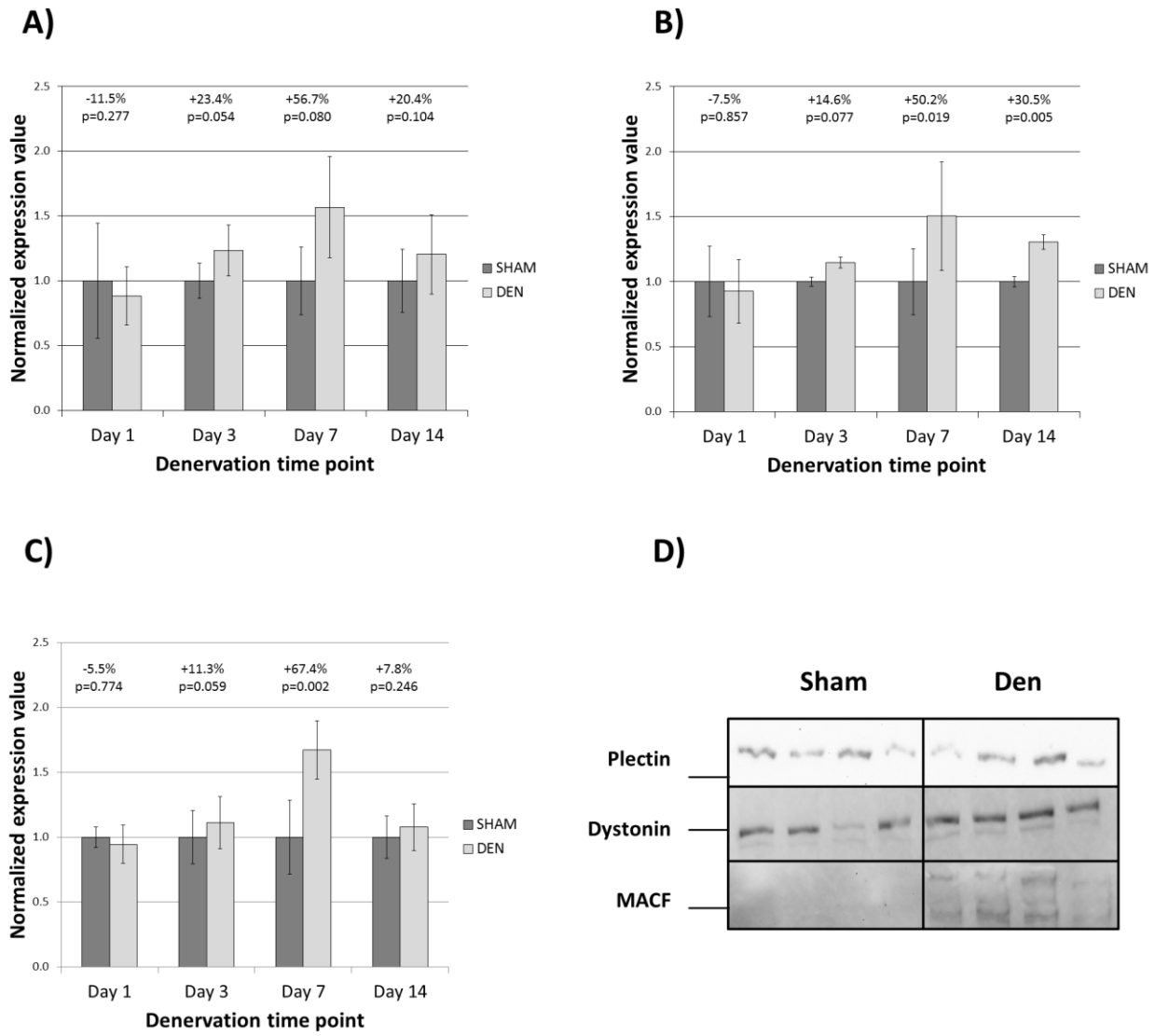

Figure 3-11: Impact of denervation on plectin, dystonin and MACF protein expression levels. Densitometry data presented in panels A, B and C are expressed as mean ± SE with den samples being normalized to a sham value of 1 (n = 8 for sham and for den for each time point, except plectin day 1 where n=6 due to the removal of two outliers). **A)** For plectin, paired samples t-tests were performed and no statistically significant differences in protein levels were found at any time point**. B)** For dystonin, a moderate upregulation was noted at day 7 (50% increase, p=0.019) and persisted through day 14 (30% increase, p=0.005). **C)** For MACF a statistically significant upregulation was found at day 7 (67.4% increase, p=0.002) but this increase was transient as protein expression levels were not found to be significant at day 14 (7.8% increase, p=0.246). **D)** Examples of Day 14 immunoblots for plectin, dystonin and MACF, with sham

samples on the right and corresponding den samples to the left. The line to the left of each blot indicates the location of the 460kDa band. All other immunoblots are displayed in Appendix B.

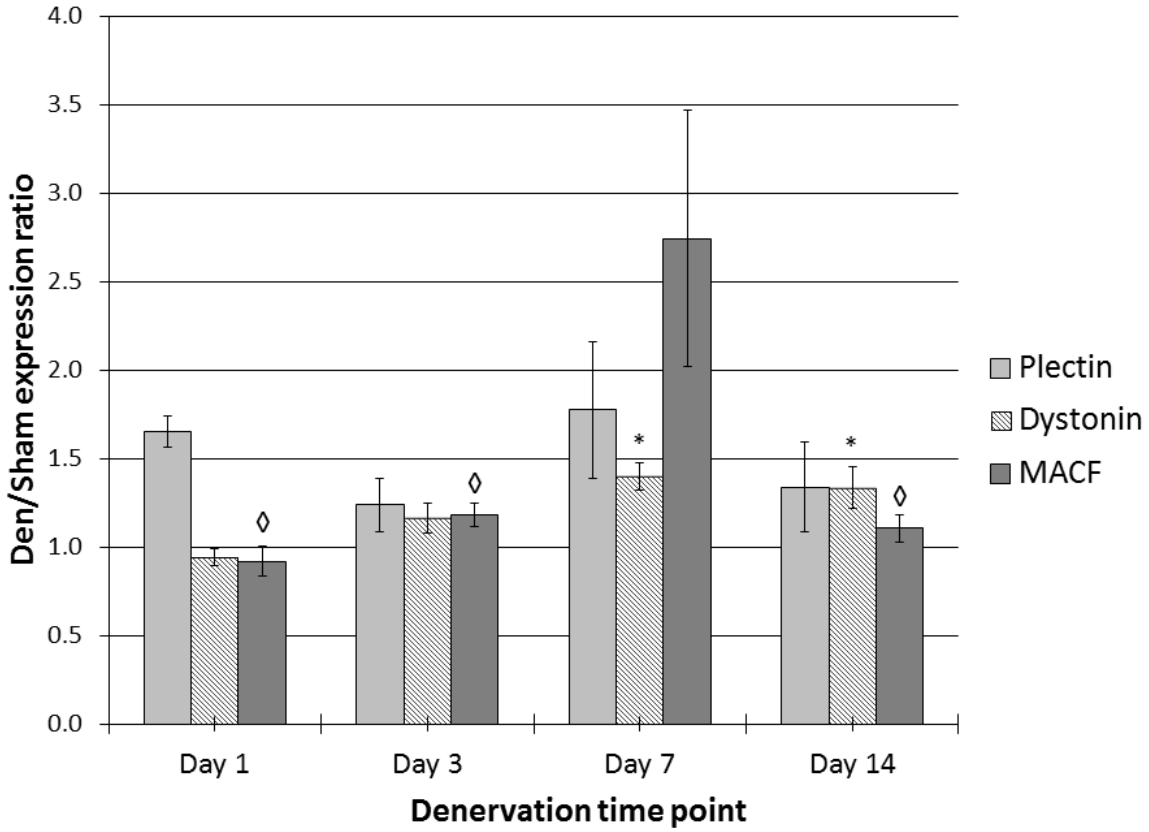

Figure 3-12: Impact of denervation on plectin, dystonin and MACF protein expression levels. Data are expressed as a ratio of protein levels in den vs sham muscles (mean ± SE) (n = 8 for den/sham ratio for each time point, except plectin where n = 6 due to the removal of outliers). Bars marked with an asterisk indicate values that are significantly different from Day 1 expression levels. Bars marked with a diamond indicate values that are significantly different from Day 7 expression levels. No statistically significant differences were observed for plectin protein expression between all denervation time points. Dystonin protein expression was slightly higher at days 7 and 14 post-denervation compared to Day 1 expression levels but the ratios were less than 1.5. MACF protein levels were significantly upregulated at day 7 but this increased expression was only transient as protein levels returned to sham levels at day 14 post-denervation.

Chapter 4

4. Discussion

The main objective of this study was to determine how the gene expression of muscle plakin family members (dystonin, plectin and MACF) is impacted by neuromuscular inactivation. We used the denervation model which is the most extreme model of inactivation because it ensures that all aspects of communication between the motor neuron (i.e. electrical activation and neurotrophic) are interrupted.

4.1. Baseline measurements - muscle atrophy and myogenin/AChE expression

Consistent with previous studies (Chen et al. 2005; Hyatt et al. 2003; Sacheck et al. 2007), we observed a 10% decrease in mouse gastrocnemius weight after three days of denervation and an approximately 40% decrease in muscle weight after fourteen days of denervation. In two studies of rat gastrocnemius, very similar results were obtained where muscle mass was reduced by 15% after three days of denervation and 55% after fourteen days (Sacheck et al. 2007; Hyatt et al. 2003). The degree of atrophy in rat is greater than we observed in mouse, but this is likely attributable to the species difference. In rat gastrocnemius muscle weight has been reported to be reduced by approximately 75% after roughly a month of denervation (Hyatt et al. 2003; Sacheck et al. 2007) but in mouse models with a similar denervation period, gastrocnemius muscle weight was reduced by 60% (Zhang et al. 2008). Our experiment did not include a denervation period of four weeks so we are unable to contrast our results with Zhang et al., (2008) but the above comparison between the studies of Zhang et al. and Hyatt et al. further corroborates a reduced severity of muscle mass loss in mouse gastrocnemius when compared to rat gastrocnemius. The difference in reaction between rat

and mouse following denervation appears fairly widespread. Physiological differences causing it could be as simple as a difference in fiber type composition, or more complex and linked to fundamental differences in gene expression patterns following denervation causing mouse muscle to be more "robust", at least when comparing atrophy (see above) and protein expression (see below – myogenin expression). As such, we are confident in our muscle weight measurements and our denervation protocol, the latter of which was doubly confirmed by measuring myogenin/AChE expression.

Myogenin expression was measured at the mRNA level through qPCR analysis in the present study. As expected, myogenin was observed to be significantly upregulated following denervation-induced atrophy, in line with previous studies (Buonanno et al. 1993; Adams et al. 1995; Eftimie et al. 1991). Buoanno et al. (1993) observed a ~100 fold increase in myogenin expression in denervated rat hindlimb muscle after ten days while we only observed a ~13 fold increase in myogenin expression in mouse gastrocnemius muscle after 14 days. The same group observed a ~40 fold increase in myogenic expression in rat soleus muscle after 2 days of denervation (Eftimie et al. 1991) while at 3 days we only observed a 10 fold increase. However, Buanno et al. (1993) reported a 10 fold increase in myogenin expression after one day of denervation in rat which is exactly what we observed in mouse. A few factors may account for these differences at varying time points. **1)** Species differences – rat muscles might respond differently to denervation than mouse muscle (i.e. rat muscles may be less tolerant of inactivation). **2)** Muscle differences – we analyzed gastrocnemius muscle in our study while in Eftimie et al. (1991) analyzed soleus muscle and in 1993 this same group of researchers analyzed the following four rat hindlimb muscles: Soleus, Extensor Digitorum Longus,

Gastrocnemius and Tibialis Anterior, although it is unclear specifically which muscle was used to quantify myogenin upregulation. It has been shown that fast and slow twitch muscle fibers have different gene expression profiles, and hindlimb muscles contain different combinations of fast and slow-twitch fibers. Gastrocnemius muscle is composed mostly of fast twitch fibers, while soleus is predominantly comprised of slow twitch muscle fibers (Burkholder et al. 1994). This difference in fiber type and distribution could account for some of the variance observed. **3)** Normalization controls – The two studies discussed above used actin as a control. As seen in Figure 2-2 we observed large variability in actin expression at day 7. Interestingly, they observed a slight decrease in actin at 7 days (Eftimie et al. 1991). In the present study, we observed that RPS12 was a more stable normalization control, and this may account for some of the differences in fold change in gene expression observed in our results. **4)** Experimental method – the above studies used northern blotting to quantify myogenin expression whereas we used qPCR. While both are reliable methods of mRNA quantitation, this difference in methodology could account for part of the variation in RNA levels observed between our study and other studies. qPCR is a more sensitive RNA quantitation method and can therefore detect more subtle differences whereas northern blotting is generally considered the standard method. This experimental difference cannot account for a similar difference noted in a more recent study which also used qPCR (MacPherson et al. 2011). MacPherson et al. showed a 30-fold increase in myogenin expression in mice after 3 days of denervation, where we only observed a 10-fold increase. However, in that study, the data were normalized to actin; in addition it is unclear from the publication which muscles were used for mRNA analyses.

As an additional control measure, the expression of AChE was also measured at the mRNA level through qPCR analysis. We found AChE expression to be downregulated following denervation induced atrophy and this is also in line with previous reports (Sketelj et al. 1998; Pregelj et al. 2007; Boudreau-Larivière et al. 2000). Our AChE expression data are similar to what has been reported in the literature. After 24 hours, a 70% reduction was reported in denervated mouse extensor digitorum longus (EDL) muscle (Sketelj et al. 1998) similarly, we observed a 61% reduction in the gastrocnemius muscle. Pregelj et al. showed an 80% reduction in AChE expression after 5 days in mouse EDL muscle (Pregelj et al. 2007), which is also comparable to our 85% reduction noted after 3 and 7 days. In rats however, the difference was slightly more pronounced with a 90% reduction after two days (Boudreau-Larivière et al. 2000). When comparing our results to those of researchers who used an identical rodent model along with very similar muscles (EDL and Gastrocnemius are both fast-twitch), the results obtained are very comparable.

It is difficult to determine exactly why our study found a less pronounced upregulation in myogenin expression compared to other studies. However, a 10-fold increase in gene expression after 24 hours is large and in that respect, consistent with the current literature. Combined with our muscle atrophy data and our AChE expression data (downregulation), collectively these findings are consistent with what has been reported in the literature by various research groups to date.

4.2. Impact of denervation on skeletal muscle plakin expression

The extent to which plectin, MACF and dystonin expression is affected in skeletal muscles that have undergone denervation-induced neuromuscular inactivation has not been extensively documented in the literature. We therefore conducted a series of qPCR and western blot experiments to measure the mRNA and protein levels of these plakin family members in control versus denervated muscles. Different trends were observed for each of these three plakins.

At the mRNA level, plectin was progressively downregulated over the denervation time course, leading to a 46% reduction in expression after seven days and a 58% reduction after fourteen days. However, we were unable to detect differences in plectin expression at the protein level at any of the denervation time points. In comparison, dystonin showed an inverse pattern when comparing mRNA and protein. At the mRNA level, dystonin expression was gradually downregulated similar to plectin but with a 50% decrease in expression after fourteen days. At the protein level, dystonin protein was upregulated by approximately 50% at 7 days post-denervation, which tapered down to a 30% increase in expression after fourteen days. Finally, the change in MACF mRNA and protein was similar but slightly different in magnitude. In particular both mRNA and protein expression peaked after seven days of denervation but mRNA showed a 2.5 fold increase at day seven, while protein expression was enhanced by 67%. We were unable to detect significant upregulation in MACF protein expression at any other time point, but mRNA showed a roughly two-fold increase at days 3 and 14 without significant upregulation after 24 hours of denervation.

4.2.1. Imperfect link between mRNA and protein expression

Although mRNA and protein expression are clearly linked with activation of DNA transcription and translation, the trends within each group are not necessarily obvious and/or co-directional. This is particularly relevant when looking at changes induced in muscle denervation, as the magnitude and duration of the up- or down-regulation of each may not coincide.

First, following denervation, the expression of genes and their products are usually found to change co-directionally (i.e. both mRNA and protein upregulated, or both downregulated). Utrophin, for example, has been shown to be upregulated both at the mRNA and protein level in denervated rodent muscle (Jasmin et al. 1995). This is similar to our MACF expression data but in contrast to our dystonin results, where a decrease in mRNA was observed along with an increase in protein expression.

Widespread changes in mRNA expression in skeletal muscle following denervation have been documented. Batt et al. (2006) used microarray analysis to survey the expression of thousands of genes. They found hundreds of examples of downregulated and upregulated genes following denervation lasting 30 and 90 days (Batt et al. 2006), which included MACF with a 3-fold upregulation in denervated muscle compared to innervated muscle. However, changes in dystonin and plectin were not reported which may suggest that changes in dystonin and plectin gene expression were not detected in the denervated muscle. While the biological relevance of this data was questioned by the authors, it does provide evidence of the magnitude of dysregulation in denervated muscle (Batt et al. 2006), at least at the mRNA level.

While mRNA expression can be linked to protein expression, this is not always the case. Gene expression is very complex and the journey from mRNA to protein can be affected by a large number of post-translational processes that can affect mRNA stability (Ross 1995), or where translation is affected by microRNAs which can affect translational efficiency (Greenbaum et al. 2003; Baek et al. 2008). A study which attempted to correlate mRNA and protein expression during growth in yeast found a large amount of variability and claimed that it is not possible to deduce protein expression through mRNA expression (Gygi et al. 1999). For example, some mRNAs were found to be stable but lead to a 20 fold difference in protein expression, while the reverse was also true: stable protein expression for certain genes was the product of mRNA expression which could vary by up to 30 fold (Gygi et al. 1999). While Gygi and colleagues (1999) suggest that the correlation between mRNA and protein is usually positive, this correlation is very weak and there are cases of extreme variability. While the Gygi et al. (1999) study was attempting to establish whether protein expression could be measured indirectly through the much simpler method of mRNA quantification, it does show that the expression levels between mRNA and protein are not 1:1 and that differences in these two biomolecules should be expected.

Like gene transcription and mRNA translation, protein dysregulation following denervation is common. For example, one study of protein expression found an upregulation of dystrophin and two dystrophin associated proteins, β-dystroglycan and adhalin, after two weeks of denervation in rat skeletal muscles using western blot analysis (Biral et al. 1996). Dystrophin was increased 1.5x and β-dystroglycan by 2.5x in their study, but due to the low abundance of adhalin in control muscle the upregulation could not be accurately measured

(Biral et al. 1996). We report a similar effect in our MACF results, where this plakin family member MACF was almost undetectable in control muscle (see Appendix B), which likely contributed to the difficulty in quantifying the increase in expression.

The change in mRNA expression without a change in protein expression, as we observed for plectin, is therefore unsurprising. The more striking difference is dystonin upregulation at the protein level but a downregulation at the mRNA level. One possible explanation is that dystonin protein is somehow resistant to degradation (i.e. proteolysis) following denervation. Either through a lowered abundance of proteases which affect dystonin, or a potential upregulation of (speculated) proteins which could interact with dystonin to protect against degradation, the half-life of dystonin in denervated muscle would be in some way increased. In this case, it would have to be significantly increased to counteract the lowered abundance of mRNA transcripts. Since dystonin mRNA levels showed a progressive decrease in expression while dystonin protein expression peaked at 7 days and decreased afterwards, it seems even the proposed transient increase in half-life of dystonin protein would not be sufficient to counteract progressively lowered mRNA transcript abundance. However, we did not measure the half-life of dystonin protein directly, and to our knowledge the half-life of dystonin has not been reported in the literature, therefore these arguments are speculative. The other important consideration is that the 30-50% increase in dystonin protein expression post-denervation would constitute a marginal change in protein expression and the extent to which this alteration has any substantial physiological relevance remains an open question. Finally, MACF showed a more classic example of a positive correlation between mRNA and protein

expression and given that the magnitude of enhanced expression exceeds a 2-fold change, this could be considered more physiologically relevant.

4.2.2. Comparison of plakins with proteins known to be dysregulated following denervation

As was discussed in the Chapter 1, denervation is known to cause widespread dysregulation in gene expression (mRNA and protein). For example, in rats, the levels of calpain-3, MHC IIB and MSE mRNA were shown to be downregulated while TRAP-2 and Glutamine synthetase were found to be upregulated in skeletal muscles denervated for 5 days (Tang et al. 2000). Proteins such as desmin, tubulin (i.e. microtubule subunit) and titin are also differentially regulated following denervation: desmin and tubulin are upregulated and titin is downregulated (Tews et al. 1997; Boudriau et al. 1996; Chen et al. 2005). A study by Magnusson and colleagues (2005) used high throughput microarray analysis to analyze gene expression in adult mouse muscle denervated for up to 6 days. They found 116 upregulated genes and 89 downregulated genes with fairly strict inclusion criteria: 2x or 0.5x expression, respectively (Magnusson et al. 2005). Interestingly, one of the upregulated genes was in fact MACF whereby a 3 fold increase was reported in the supplemental information document of this article (Magnusson et al. 2005). By applying similar criteria (i.e. minimum 2 fold increase and 0.5 fold decrease) to the present study, our plectin, dystonin and MACF mRNA expression data would be considered significantly different in denervated compared to innervated muscle.

4.2.3. Implications of the plectin, dystonin and MACF expression profile in denervated muscle.

Plectin and dystonin reacted similarly to denervation compared to MACF. They were both downregulated at the mRNA level while MACF was upregulated at the mRNA level. At the protein level, however, plectin and dystonin seemed to resist downregulation with dystonin being slightly upregulated. This resistance to downregulation at the protein level might be important to preserve muscle fiber integrity following short term denervation. It has been shown that re-innervation after a short period of denervation (<7 days) reverses all changes in the muscle and longer denervation periods impair recovery, although recovery is still possible to some extent even after months of denervation (Finkelstein et al. 1993; Irintchev et al. 1990). We did not measure plakin expression beyond 2 weeks of denervation, but it is possible that the fairly stable dystonin and plectin protein expression after short-term denervation would contribute to the described recovery during re-innervation. Dystonin and plectin are large architectural proteins which may have partial functional redundancy (Boudreau-Larivière & Kothary 2002). For instance, as described in Chapter 1, dystonin and plectin share similar functions such as binding to mitochondria and to the Z-line in muscle. In fact, the muscle isoform of dystonin binds to plectin through their mutual actin binding domains, and in plectin null mice dystonin is less abundant due to this association (Steiner-Champliaud et al. 2010). However, they are also functionally distinct in some respects. For example, the muscle-specific isoforms of dystonin show no binding to desmin where plectin readily binds to desmin (Steiner-Champliaud et al. 2010). Whether or not this functional similarity and protein co-localization contributes to the similarities observed in dystonin and plectin expression following denervation remains an open question. Due to their demonstrated binding activity (Steiner-

Champliaud et al. 2010), it could be argued that their expression at the protein level is not independent. One possibility is that the binding of dystonin to plectin would affect its stability post-denervation and this could explain their relative stability. Further research is required to assess if this stability is affected by the binding of plectin and dystonin, and to assess the effect that heightened dystonin and stable plectin protein expression has on the ability of denervated muscle to recover following re-innervation.

MACF is considered to be a developmental protein in muscle tissue. MACF was found to be highly expressed in the nervous system, skin and skeletal muscle of embryonic day-17.5 mice, as well as in the lung of mice right before birth (Bernier et al. 2000). However, even three days post-natal, MACF expression in muscle is significantly reduced while it remains strongly expressed in the nervous system, skin and lungs (Bernier et al. 2000). Many other genes are differentially regulated during development. For example, some Muscle Ring Finger proteins (MuRFs), specifically MuRF2, have been shown to be downregulated post-natally (Perera et al. 2012). The 50kDa isoform of MuRF2, while highly expressed at embryonic day 15.5, is almost undetectable in adult muscle while the 60kDa isoform is heavily expressed shortly after birth but much less expressed in adult muscle (Perera et al. 2012). Other examples are nAChRs which exists in two isoforms, AChR-γ and AChR-ε. The gamma variant is also known as the embryonic-type AChR; it is expressed during development but is downregulated and replaced by AChR-ε in adult muscle (Witzemann et al. 2013).

Following denervation, the expression of these genes in muscle returns to their developmental expression. MURFs have been shown to be upregulated following denervation

(Glass & Roubenoff 2010). The same happens with nAChRs, where following denervation the AChR-ε that are expressed in adult skeletal muscle are replaced with AChR-γ normally found in developing muscle (Gu & Hall 1988). During development, muscle tissue growth occurs independent of innervation. It is only later that nerves form synapses with the muscle fibers. This innervation alters the physiology of the muscle and is an integral part of muscle development (MacIntosh et al. 2006). As already stated, it seems that denervation reverts muscle to an embryonic state, rebooting the developmental expression profile. This is consistent with what we observed with MACF, where denervation increases expression of a protein, which is not normally expressed in adult muscle, but is more highly expressed in developing muscle (Bernier et al. 2000).

In the case of acetylcholine receptors, described above, the expression is transient similar to what we have shown for MACF. In wild-type mice, the expression of embryonic AChRs induced by denervation peaks roughly 5 days post-denervation. Afterwards, embryonic AChRs degrade and are replaced by adult AChRs, returning to innervated levels after about 20 days (Yampolsky et al. 2010). We did not measure MACF expression following 20 days of denervation, but we did observe a decrease in expression after 14 days relative to the peak expression at seven days. It is not known whether or not MACF would return to baseline levels of expression after a sufficiently long period of time.

Also remaining to be elucidated is determining the physiological implications of enhanced MACF expression in denervated muscles that are atrophying. Does it represent a functional, transient adaptation in denervated muscle fibers whereby MACF offers additional

stabilizing support to other plakin family members (i.e. Plectin, dystonin structures)? Alternatively, is the enhanced MACF expression simply reflecting a shift in the gene expression programming towards one that recapitulates embryonic development or a combination of the two possibilities? One strategy to address this point would be to generate muscle-specific MACF knockout mice and to study the skeletal muscle phenotype (muscle mass and gene expression profile) of these animals post-denervation. It would be of interest to determine whether muscle atrophy would be exacerbated, minimized or comparable to control animals. This knockout model might also shed light on the nerve-activity induced expression of MACF. In normal muscle, if MACF is upregulated due to muscle reverting in some way to an embryonic expression profile, MACF might be powerless to affect atrophy, positively or negatively, in its transiently expressed state because it is not adapted to function in adult muscle. In a theoretical MACF knockout model, any worsening of atrophy would disprove this, implying that MACF upregulation may be relevant to the functioning of muscle post-denervation.

Chapter 5

5. Conclusion

We expected a downregulation in plectin and dystonin at both the protein and mRNA level in denervated muscle, as well as an upregulation of MACF at the protein and mRNA level. What we found was a downregulation of plectin and dystonin mRNA but either stable or slightly upregulated protein expression for plectin and dystonin respectively. For MACF the results were as expected, confirming previous data showing an upregulation at the mRNA level (Magnusson et al. 2005) but also demonstrating an upregulation at the protein level. These results help shed light on the gene expression profile of the skeletal muscle plakins during denervation-induced atrophy, providing more examples of critical structural proteins that are dysregulated during this type of atrophy.

5.1. Limitations

This study provided some insight into expression levels of plakin proteins following hindlimb denervation in mice. One limitation is that the primers used for the qPCR and the antibodies used for the western blotting do not allow us to determine the impact of neuromuscular inactivation on the various individual plectin, dystonin and MACF isoforms predominantly expressed in skeletal muscle. Our mRNA and protein expression data are rather an overall expression profile of each plakin family member. Furthermore, the results have to be taken in the context of the fairly small sample size of mice (n=8) used. While in line with many other rodent studies, the small number of animals used reduces the statistical power, especially when considering the high variance western blot data. High molecular weight western blotting is a standard method for assessing protein expression, and while large changes can be observed

in the data, other more subtle trends can be missed. Finally, our data do not allow us to determine the exact underlying molecular mechanisms that lead to the changes in mRNA and protein expression of the target plakins (i.e. transcriptional vs post-transcriptional mechanisms).

5.2. Future Directions

Further studies on plakin protein expression in denervated muscle could involve the development of mice with a conditional MACF knockout in muscle (as MACF knockouts are embryonic lethal). This knockout could be used to assess the roles of MACF in postnatal development, if any exist. Specifically relating to denervation, a conditional MACF knockout in muscle would allow us to evaluate the role of MACF following denervation. Its marked upregulation, while likely a direct result of the lack of neural activity, could have no regulatory or structural role, or perhaps MACF upregulation does serve some role in denervated muscle and the upregulation following denervation is beneficial.

Short of developing a conditional MACF knockout mouse, further studies on plakin expression following denervation that are isoform-specific could shed light on the denervation-related regulatory and structural role of various isoforms. For example, what isoforms of plectin that are expressed in muscle are affected more or less during denervation. Perhaps plectin 1d and 1f are upregulated while plectin 1b, which affect mitochondrial stability, are less important when neural activity is inhibited. In this case some plectin variants would be upregulated while some are downregulated, leading to our observed stable expression. It is also possible that all isoforms of plectin (and other muscle plakins within the same family) are affected similarly following denervation. Only isoform specific studies could determine this.

Future studies could also be conducted to determine the impact of skeletal muscle hypertrophy on the expression profile of plectin, dystonin, and MACF isoforms by using a surgical intervention such as tenotomy of hindlimb muscle whereby all tendons except that of one muscle, typically that of the plantaris, is left intact thereby leaving the plantaris to take on the entire load of foot flexion. It would be interesting to see if enhanced neuromuscular activity leading to muscle hypertrophy would impact plakin expression.

References

Ackerl, R. et al., 2007. Conditional targeting of plectin in prenatal and adult mouse stratified epithelia causes keratinocyte fragility and lesional epidermal barrier defects. *Journal of Cell Science*, 120, pp.2435–2443.

Adams, L. et al., 1995. Adaptation of nicotinic acetylcholine receptor, myogenin, and MRF4 gene expression to long-term muscle denervation. *The Journal of cell biology*, 131(5), pp.1341–9. Available at: http://www.pubmedcentral.nih.gov/articlerender.fcgi?artid=2120634&tool=pmcentrez&rendertype=abstract.

Andra, K. et al., 1997. Targeted inactivation of plectin reveals essential function in maintaining the integrity of skin, muscle, and heart cytoarchitecture. *Genes & Development*, 11(23), pp.3143–3156. Available at: http://www.genesdev.org/cgi/doi/10.1101/gad.11.23.3143 [Accessed May 1, 2012].

Applewhite, D.A. et al., 2010. The Spectraplakin Short Stop Is an Actin – Microtubule Cross-Linker That Contributes to Organization of the Microtubule Network. , 21, pp.1714–1724.

Baek, D. et al., 2008. The impact of microRNAs on protein output. *Nature*, 455(7209), pp.64–71. Available at: http://www.nature.com/nature/journal/v455/n7209/pdf/nature07242.pdf [Accessed July 12, 2014].

Bang, M.L. et al., 2001. The complete gene sequence of titin, expression of an unusual approximately 700-kDa titin isoform, and its interaction with obscurin identify a novel Z-line to I-band linking system. *Circulation research*, 89, pp.1065–1072.

Batt, J. et al., 2006. Differential gene expression profiling of short and long term denervated muscle. *FASEB journal : official publication of the Federation of American Societies for Experimental Biology*, 20(1), pp.115–7. Available at: http://www.ncbi.nlm.nih.gov/pubmed/16291642.

Bernier, G. et al., 2000. Acf7 (MACF) is an actin and microtubule linker protein whose expression predominates in neural, muscle, and lung development. *Developmental dynamics : an official publication of the American Association of Anatomists*, 219(2), pp.216–25. Available at: http://www.ncbi.nlm.nih.gov/pubmed/11002341.

Biral, D., Senter, L. & Salviati, G., 1996. Increased expression of dystrophin, beta-dystroglycan and adhalin in denervated rat muscles. *Journal of Muscle Research and Cell Motility*, 17(5), pp.523–532. Available at: http://link.springer.com/10.1007/BF00124352 [Accessed May 22, 2015].

Bodine, S.C. et al., 2001. Identification of ubiquitin ligases required for skeletal muscle atrophy. *Science (New York, N.Y.)*, 294(5547), pp.1704–8. Available at: http://www.ncbi.nlm.nih.gov/pubmed/11679633.

Booth, F.W. & Kelso, J.R., 1973. Production of rat muscle atrophy by cast fixation. *J Appl Physiol*, 34(3), pp.404–406. Available at: http://jap.physiology.org/content/34/3/404 [Accessed September 19, 2015].

Bosher, J.M. et al., 2003. The Caenorhabditis elegans vab-10 spectraplakin isoforms protect the epidermis against internal and external forces. *The Journal of cell biology*, 161(4), pp.757–68. Available at: http://www.pubmedcentral.nih.gov/articlerender.fcgi?artid=2199363&tool=pmcentrez&rendertype=abstract [Accessed February 27, 2013].

Bouameur, J.-E., Favre, B. & Borradori, L., 2014. Plakins, a versatile family of cytolinkers: roles in skin integrity and in human diseases. *The Journal of investigative dermatology*, 134(4), pp.885–94. Available at: http://www.ncbi.nlm.nih.gov/pubmed/24352042.

Boudreau-Larivière, C. et al., 2000. Molecular mechanisms underlying the activity-linked alterations in acetylcholinesterase mRNAs in developing versus adult rat skeletal muscles. *Journal of neurochemistry*, 74(6), pp.2250–8. Available at: http://www.ncbi.nlm.nih.gov/pubmed/10820184.

Boudreau-Larivière, C. & Kothary, R., 2002. Differentiation potential of primary myogenic cells derived from skeletal muscle of dystonia musculorum mice. *Differentiation*, 70(6), pp.247–256.

Boudriau, S. et al., 1996. Remodeling of the cytoskeletal lattice in denervated skeletal muscle. *Muscle & nerve*, 19(11), pp.1383–90. Available at: http://www.ncbi.nlm.nih.gov/pubmed/8874395.

Boyer, J.G., Bernstein, M. a & Boudreau-Larivière, C., 2010. Plakins in striated muscle. *Muscle & nerve*, 41(3), pp.299–308. Available at: http://www.ncbi.nlm.nih.gov/pubmed/19768769 [Accessed May 1, 2012].

Braun, T. & Gautel, M., 2011. Transcriptional mechanisms regulating skeletal muscle differentiation, growth and homeostasis. *Nature reviews. Molecular cell biology*, 12(6), pp.349–361. Available at: http://dx.doi.org/10.1038/nrm3118.

Buonanno, A., Edmondson, D.G. & Hayes, W.P., 1993. Upstream sequences of the myogenin gene convey responsiveness to skeletal muscle denervation in transgenic mice. *Nucleic acids research*, 21(24), pp.5684–5693.

Burkholder, T.J. et al., 1994. Relationship between muscle fiber types and sizes and muscle architectural properties in the mouse hindlimb. *Journal of morphology*, 221(2), pp.177–190.

Capetanaki, Y. et al., 2007. Muscle intermediate filaments and their links to membranes and membranous organelles. *Experimental Cell Research*, 313, pp.2063–2076.

Carlson, B.M. & Billington, L., 1996. Studies on the regenerative recovery of long-term denervated muscle in rats. *Restorative neurology and Neuroscience*, 10, pp.77–84. Available at: http://iospress.metapress.com/index/U6114M57N4336751.pdf [Accessed May 15, 2012].

Carlson, B.M. & Faulkner, J. a, 1988. Reinnervation of long-term denervated rat muscle freely grafted into an innervated limb. *Experimental neurology*, 102(1), pp.50–6. Available at: http://www.ncbi.nlm.nih.gov/pubmed/3181352.

Castañón, M.J. et al., 2013. Plectin-intermediate filament partnership in skin, skeletal muscle, and peripheral nerve. *Histochemistry and cell biology*, 140(1), pp.33–53. Available at: http://www.pubmedcentral.nih.gov/articlerender.fcgi?artid=3695321&tool=pmcentrez&rendertype=abstract [Accessed September 3, 2013].

Chatzifrangkeskou, M., Bonne, G. & Muchir, A., 2015. Nuclear envelope and striated muscle diseases. *Current Opinion in Cell Biology*, 32, pp.1–6. Available at: http://linkinghub.elsevier.com/retrieve/pii/S0955067414001185.

Chen, H.-J. et al., 2006. The role of microtubule actin cross-linking factor 1 (MACF1) in the Wnt signaling pathway. *Genes & development*, 20(14), pp.1933–45. Available at: http://www.pubmedcentral.nih.gov/articlerender.fcgi?artid=1522081&tool=pmcentrez&rendertype=abstract [Accessed June 1, 2013].

Chen, S.P. et al., 2005. Decline in titin content in rat skeletal muscle after denervation. *Muscle and Nerve*, 32(6), pp.798–807.

Clark, K. a et al., 2002. Striated muscle cytoarchitecture: an intricate web of form and function. *Annual review of cell and developmental biology*, 18, pp.637–706.

Cohen, T.J. et al., 2007. The histone deacetylase HDAC4 connects neural activity to muscle transcriptional reprogramming. *The Journal of biological chemistry*, 282(46), pp.33752–9. Available at: http://www.ncbi.nlm.nih.gov/pubmed/17873280 [Accessed March 14, 2012].

Dalpé, G. et al., 1999. Dystonin-deficient mice exhibit an intrinsic muscle weakness and an instability of skeletal muscle cytoarchitecture. *Developmental biology*, 210(2), pp.367–80. Available at: http://www.ncbi.nlm.nih.gov/pubmed/10357897.

Dominiguez, R. & Holmes, K., 2011. NIH Public Access. *Annu Rev Biophys. 2011 Jube 9; 40: 169-186.doi:10.1146/annurev-biophys-042910-155359*, (3), pp.169–186.

Dow, D.E. et al., 2004. Number of contractions to maintain mass and force of a denervated rat muscle. *Muscle & nerve*, 30(1), pp.77–86. Available at: http://www.ncbi.nlm.nih.gov/pubmed/15221882 [Accessed March 23, 2012].

Eftimie, R., Brenner, H.R. & Buonanno, A., 1991. Myogenin and MyoD join a family of skeletal muscle genes regulated by electrical activity. *Proceedings of the National Academy of Sciences of the United States of America*, 88(4), pp.1349–53. Available at: http://www.pubmedcentral.nih.gov/articlerender.fcgi?artid=51015&tool=pmcentrez&rendertype=abstract.

Erickson, H.P., 2007. Evolution of the cytoskeleton. *BioEssays : news and reviews in molecular, cellular and developmental biology*, 29(7), pp.668–77. Available at: http://www.pubmedcentral.nih.gov/articlerender.fcgi?artid=2630885&tool=pmcentrez&rendertype=abstract [Accessed March 4, 2013].

Faulkner, G., Lanfranchi, G. & Valle, G., 2001. Telethonin and other new proteins of the Z-disc of skeletal muscle. *IUBMB life*, 51, pp.275–282.

Ferrier, A., Boyer, J.G. & Kothary, R., 2013. *Cellular and Molecular Biology of Neuronal Dystonin.*, Elsevier. Available at: http://www.ncbi.nlm.nih.gov/pubmed/23273860 [Accessed January 8, 2013].

Finkelstein, D.I., Dooley, P.C. & Luff, A.R., 1993. Recovery of muscle after different periods of denervation and treatments. *Muscle & nerve*, 16(7), pp.769–77. Available at: http://www.ncbi.nlm.nih.gov/pubmed/8505933 [Accessed June 16, 2015].

Fuchs, P. et al., 1999. Unusual 5’ transcript complexity of plectin isoforms: novel tissue-specific exons modulate actin binding activity. *Human molecular genetics*, 8(13), pp.2461–72. Available at: http://www.ncbi.nlm.nih.gov/pubmed/10556294.

Glass, D. & Roubenoff, R., 2010. Recent advances in the biology and therapy of muscle wasting. *Annals of the New York Academy of Sciences*, 1211, pp.25–36.

Glass, D.J., 2005. Skeletal muscle hypertrophy and atrophy signaling pathways. *The international journal of biochemistry & cell biology*, 37(10), pp.1974–84. Available at: http://www.ncbi.nlm.nih.gov/pubmed/16087388 [Accessed June 1, 2013].

Goryunov, D. et al., 2010. Nervous-Tissue-Specific Elimination of Microtubule-Actin Crosslinking Factor 1a Results in Multiple Developmental Defects in the Mouse Brain. *Mol Cell Neurosci*, 44(1), pp.1–14.

Greenbaum, D. et al., 2003. Comparing protein abundance and mRNA expression levels on a genomic scale. *Genome biology*, 4(9), p.117.

Gu, Y. & Hall, Z.W., 1988. Immunological evidence for a change in subunits of the acetylcholine receptor in developing and denervated rat muscle. *Neuron*, 1(2), pp.117–125. Available at: http://www.sciencedirect.com/science/article/pii/089662738890195X [Accessed June 14, 2015].

Gygi, S.P. et al., 1999. Correlation between protein and mRNA abundance in yeast. *Molecular and cellular biology*, 19(3), pp.1720–1730.

Hasselgren, P.O. & Fischer, J.E., 2001. Muscle cachexia: current concepts of intracellular mechanisms and molecular regulation. *Annals of surgery*, 233(1), pp.9–17.

Hijikata, T. et al., 1999. Plectin is a linker of intermediate filaments to Z-discs in skeletal muscle fibers. *Journal of cell science*, 112(6), pp.867–76. Available at: http://www.ncbi.nlm.nih.gov/pubmed/10036236.

Hoppeler, H. & Fluck, M., 2003. Plasticity of skeletal muscle mitochondria: structure and function. *Medicine and science in sports and exercise*, 35(August 2002), pp.95–104.

Hyatt, J.-P.K. et al., 2003. Nerve activity-independent regulation of skeletal muscle atrophy: role of MyoD and myogenin in satellite cells and myonuclei. *American journal of physiology. Cell physiology*, 285, pp.C1161–C1173.

Irintchev, A., Draguhn, A. & Wernig, A., 1990. Reinnervation and recovery of mouse soleus muscle after long-term denervation. *Neuroscience*, 39(1), pp.231–243. Available at: http://www.sciencedirect.com/science/article/pii/030645229090236W [Accessed June 16, 2015].

Jasmin, B.J. et al., 1995. Expression of utrophin and its mRNA in denervated mdx mouse muscle. *FEBS letters*, 374(3), pp.393–398.

Jefferson, J.J., Leung, C.L. & Liem, R.K.H., 2004. Plakins: goliaths that link cell junctions and the cytoskeleton. *Nature reviews. Molecular cell biology*, 5(7), pp.542–53. Available at: http://www.ncbi.nlm.nih.gov/pubmed/15232572 [Accessed February 7, 2013].

Kandarian, S.C. & Jackman, R.W., 2006. Intracellular signaling during skeletal muscle atrophy. *Muscle & nerve*, 33(February), pp.155–165.

Karakesisoglou, I., 2000. An epidermal plakin that integrates actin and microtubule networks at cellular junctions. *The Journal of cell biology*, 149(1), pp.195–208. Available at: http://jcb.rupress.org/content/149/1/195.short [Accessed May 16, 2012].

Karakesisoglou, I., Yang, Y. & Fuchs, E., 2000. An Epidermal Plakin that Integrates Actin and Microtubule Networks at Cellular Junctions. , 149(1), pp.195–208.

Kelleher, A.R. et al., 2013. The mTORC1 signaling repressors REDD1/2 are rapidly induced and activation of p70S6K1 by leucine is defective in skeletal muscle of an immobilized rat hindlimb. *American journal of physiology. Endocrinology and metabolism*, 304, pp.E229–36. Available at: http://www.pubmedcentral.nih.gov/articlerender.fcgi?artid=3543567&tool=pmcentrez&rendertype=abstract.

Kharraz, Y. et al., 2014. Understanding the process of fibrosis in duchenne muscular dystrophy. *BioMed Research International*, 2014.

Konieczny, P. et al., 2008. Myofiber integrity depends on desmin network targeting to Z-disks and costameres via distinct plectin isoforms. *The Journal of cell biology*, 181(4), pp.667–81. Available at: http://www.pubmedcentral.nih.gov/articlerender.fcgi?artid=2386106&tool=pmcentrez&rendertype=abstract [Accessed May 22, 2012].

Lawler, J.M., Song, W. & Demaree, S.R., 2003. Hindlimb unloading increases oxidative stress and disrupts antioxidant capacity in skeletal muscle. *Free Radical Biology and Medicine*, 35(1), pp.9–16.

Léger, B. et al., 2006. Human skeletal muscle atrophy in amyotrophic lateral sclerosis reveals a reduction in Akt and an increase in atrogin-1. *The FASEB journal : official publication of the Federation of American Societies for Experimental Biology*, 20, pp.583–585.

Leung, C. & Liem, R., 2001. The plakin family. *Journal of Cell Science*, 114(19), pp.3409–3410. Available at: http://jcs.biologists.org/content/114/19/3409.short [Accessed May 16, 2012].

Leung, C.L. et al., 2001. The BPAG1 locus: Alternative splicing produces multiple isoforms with distinct cytoskeletal linker domains, including predominant isoforms in neurons and muscles. *The Journal of cell biology*, 154(4), pp.691–7. Available at: http://www.pubmedcentral.nih.gov/articlerender.fcgi?artid=2196450&tool=pmcentrez&rendertype=abstract [Accessed May 1, 2013].

MacIntosh, B.R., Gardiner, P.F. & McComas, A.J., 2006. *Skeletal Muscle: Form and Function*, Human Kinetics. Available at: https://books.google.com/books?hl=en&lr=&id=-EfxEhSFaMYC&pgis=1 [Accessed May 18, 2015].

MacPherson, P.C.D., Wang, X. & Goldman, D., 2011. Myogenin regulates denervation-dependent muscle atrophy in mouse soleus muscle. *Journal of Cellular Biochemistry*, 112(8), pp.2149–2159.

Magnusson, C. et al., 2005. Denervation-induced alterations in gene expression in mouse skeletal muscle. *The European journal of neuroscience*, 21, pp.577–580.

Mihailovska, E. et al., 2014. Neuromuscular synapse integrity requires linkage of acetylcholine receptors to postsynaptic intermediate filament networks via rapsyn-plectin 1f complexes. *Molecular Biology of the Cell*, 25(25), pp.4130–4149. Available at: http://www.molbiolcell.org/cgi/doi/10.1091/mbc.E14-06-1174.

Mitchell, W.K. et al., 2012. Sarcopenia, dynapenia, and the impact of advancing age on human skeletal muscle size and strength; a quantitative review. *Frontiers in Physiology*, 3 JUL(July), pp.1–18.

Norgett, E.E. et al., 2000. Recessive mutation in desmoplakin disrupts desmoplakin-intermediate filament interactions and causes dilated cardiomyopathy, woolly hair and keratoderma. *Human molecular genetics*, 9(18), pp.2761–6. Available at: http://www.ncbi.nlm.nih.gov/pubmed/11063735.

Oishi, Y. et al., 2001. Expression of heat shock protein 72 in atrophied rat skeletal muscles. *Acta Physiol Scand.*, 172, pp.123–30.

Perera, S., Mankoo, B. & Gautel, M., 2012. Developmental regulation of MURF E3 ubiquitin ligases in skeletal muscle. *Journal of Muscle Research and Cell Motility*, 33(2), pp.107–122.

Phillips, S.M., 2014. A brief review of critical processes in exercise-induced muscular hypertrophy. *Sports Medicine*, 44(SUPPL.1), pp.71–77.

Picard, M., White, K. & Turnbull, D.M., 2012. Mitochondrial morphology, topology and membrane interactions in skeletal muscle: A quantitative three-dimensional electron microscopy study. *Journal of Applied Physiology*, 19104, pp.161–171.

Powers, S.K. et al., 2012. Mitochondrial signaling contributes to disuse muscle atrophy. *American journal of physiology. Endocrinology and metabolism*, 9575(352). Available at: http://www.ncbi.nlm.nih.gov/pubmed/22395111 [Accessed March 16, 2012].

Powers, S.K. et al., 2014. Oxidative stress and disuse muscle atrophy Free Radical Biology in Skeletal Muscle Oxidative stress and disuse muscle atrophy. , pp.2389–2397.

Pregelj, P. et al., 2007. The role of muscle activation pattern and calcineurin in acetylcholinesterase regulation in rat skeletal muscles. *The Journal of neuroscience : the official journal of the Society for Neuroscience*, 27(5), pp.1106–1113.

Raith, M. et al., 2013. Linking cytoarchitecture to metabolism: sarcolemma-associated plectin affects glucose uptake by destabilizing microtubule networks in mdx myofibers. *Skeletal muscle*, 3(1), p.14. Available at:

http://www.pubmedcentral.nih.gov/articlerender.fcgi?artid=3695810&tool=pmcentrez&rendertype=abstract.

Reipert, S. et al., 1999. Association of mitochondria with plectin and desmin intermediate filaments in striated muscle. *Experimental cell research*, 252(2), pp.479–91. Available at: http://www.ncbi.nlm.nih.gov/pubmed/10527638.

Rezniczek, G. a et al., 2003. Plectin 5'-transcript diversity: short alternative sequences determine stability of gene products, initiation of translation and subcellular localization of isoforms. *Human molecular genetics*, 12(23), pp.3181–94. Available at: http://www.ncbi.nlm.nih.gov/pubmed/14559777 [Accessed June 14, 2013].

Rezniczek, G. a. et al., 2007. Plectin 1f scaffolding at the sarcolemma of dystrophic (mdx) muscle fibers through multiple interactions with β-dystroglycan. *Journal of Cell Biology*, 176(7), pp.965–977.

Ross, J., 1995. mRNA stability in mammalian cells. *Microbiological reviews*, 59(3), pp.423–450.

Sacheck, J.M. et al., 2007. Rapid disuse and denervation atrophy involve transcriptional changes similar to those of muscle wasting during systemic diseases. *The FASEB journal : official publication of the Federation of American Societies for Experimental Biology*, 21(1), pp.140–155.

Sanchez-Soriano, N. et al., 2009. Mouse ACF7 and drosophila short stop modulate filopodia formation and microtubule organisation during neuronal growth. *Journal of cell science*, 122(Pt 14), pp.2534–42. Available at: http://www.pubmedcentral.nih.gov/articlerender.fcgi?artid=2704885&tool=pmcentrez&rendertype=abstract [Accessed December 8, 2012].

Sanes, J. & Lichtman, J., 2001. Induction, assembly, maturation and maintenance of a postsynaptic apparatus. *Nature Reviews Neuroscience*, 2(November). Available at: http://www.nature.com/nrn/journal/v2/n11/abs/nrn1101-791a.html [Accessed May 14, 2013].

Schroder, R. et al., 1997. Altered distribution of plectin/HD1 in dystrophinopathies. *Neuromuscular Disorders*, 7(6-7), pp.436–437. Available at: http://www.ingentaconnect.com/content/els/09608966/1997/00000007/00000006/art87203 [Accessed May 31, 2015].

Schröder, R. et al., 1999. Immunogold EM reveals a close association of plectin and the desmin cytoskeleton in human skeletal muscle. *European journal of cell biology*, 78(4), pp.288–95. Available at: http://dx.doi.org/10.1016/S0171-9335(99)80062-4 [Accessed May 14, 2013].

Sellers, J.R., 2000. Myosins: A diverse superfamily. *Biochimica et Biophysica Acta - Molecular Cell Research*, 1496(1), pp.3–22.

Sketelj, J. et al., 1998. Acetylcholinesterase mRNA level and synaptic activity in rat muscles depend on nerve-induced pattern of muscle activation. *The Journal of neuroscience : the official journal of the Society for Neuroscience*, 18(6), pp.1944–1952.

Slack, J.M., Holland, P.W. & Graham, C.F., 1993. The zootype and the phylotypic stage. *Nature*, 361(6412), pp.490–492.

Sonnenberg, A. & Liem, R.K.H., 2007. Plakins in development and disease. *Experimental cell research*, 313(10), pp.2189–203. Available at: http://www.ncbi.nlm.nih.gov/pubmed/17499243 [Accessed January 30, 2013].

Steiner-Champliaud, M.F. et al., 2010. BPAG1 isoform-b: Complex distribution pattern in striated and heart muscle and association with plectin and α-actinin. *Experimental Cell Research*, 316(3), pp.297–313. Available at: http://dx.doi.org/10.1016/j.yexcr.2009.11.010.

Strumpf, D. & Volk, T., 1998. Kakapo, a novel cytoskeletal-associated protein is essential for the restricted localization of the neuregulin-like factor, vein, at the muscle-tendon junction site. *The Journal of cell biology*, 143(5), pp.1259–70. Available at: http://www.pubmedcentral.nih.gov/articlerender.fcgi?artid=2133081&tool=pmcentrez&rendertype=abstract.

Sun, D., Leung, C.L. & Liem, R.K.H., 2000. Characterization of the microtubule binding domain of microtubule actin crosslinking factor (MACF): identification of a novel group of microtubule associated proteins.

Suozzi, K.C., Wu, X. & Fuchs, E., 2012. Spectraplakins: Master orchestrators of cytoskeletal dynamics. *The Journal of Cell Biology*, 197(4), pp.465–475. Available at: http://www.jcb.org/cgi/doi/10.1083/jcb.201112034 [Accessed May 14, 2012].

Tang, H. et al., 2000. Identification and characterization of differentially expressed genes in denervated muscle. *Molecular and cellular neurosciences*, 16(2), pp.127–140.

Tews, D.S. et al., 1997. Expression profile of stress proteins, intermediate filaments, and adhesion molecules in experimentally denervated and reinnervated rat facial muscle. *Experimental neurology*, 146(1), pp.125–134.

Thomason, D.B. & Booth, F.W., 1990. Atrophy of the soleus muscle by hindlimb unweighting. *Journal of applied physiology (Bethesda, Md. : 1985)*, 68, pp.1–12.

Timmons, J. a, 2011. Variability in training-induced skeletal muscle adaptation Signals Mediating Skeletal Muscle Remodeling by Activity Variability in training-induced skeletal muscle adaptation. , (October 2010), pp.846–853.

Trinick, J. & Tskhovrebova, L., 2010. Roles of titin in the structure and elasticity of the sarcomere. *Journal of Biomedicine and Biotechnology*, 2010, pp.1–7.

Valencia, R.G. et al., 2013. Intermediate filament-associated cytolinker plectin 1c destabilizes microtubules in keratinocytes. *Molecular biology of the cell*, 24(6), pp.768–84. Available at: http://www.pubmedcentral.nih.gov/articlerender.fcgi?artid=3596248&tool=pmcentrez&rendertype=abstract [Accessed September 3, 2013].

Wiche, G. et al., 1984. Identification of plectin in different human cell types and immunolocalization at epithelial basal cell surface membranes. *Experimental Cell Research*, 155(1), pp.43–49. Available at: http://dx.doi.org/10.1016/0014-4827(84)90766-3 [Accessed June 1, 2013].

Wiche, G., 1989. Plectin: general overview and appraisal of its potential role as a subunit protein of the cytomatrix. *Critical reviews in biochemistry and molecular biology*, 24(1), pp.41–67. Available at: http://www.ncbi.nlm.nih.gov/pubmed/2667895.

Wilson, M.H. & Holzbaur, E.L.F., 2012. Opposing microtubule motors drive robust nuclear dynamics in developing muscle cells. *Journal of cell science*, 125(Pt 17), pp.4158–69. Available at: http://www.ncbi.nlm.nih.gov/pubmed/22623723 [Accessed June 13, 2013].

Winter, L., Abrahamsberg, C. & Wiche, G., 2008. Plectin isoform 1b mediates mitochondrion - Intermediate filament network linkage and controls organelle shape. *Journal of Cell Biology*, 181, pp.903–911.

Witzemann, V. et al., 2013. The neuromuscular junction: Selective remodeling of synaptic regulators at the nerve/muscle interface. *Mechanisms of Development*, 130(6-8), pp.402–411.

Wu, X., Kodama, A. & Fuchs, E., 2008. ACF7 regulates cytoskeletal-focal adhesion dynamics and migration and has ATPase activity. *Cell*, 135(1), pp.137–48. Available at: http://www.pubmedcentral.nih.gov/articlerender.fcgi?artid=2703712&tool=pmcentrez&rendertype=abstract [Accessed March 1, 2013].

Yampolsky, P., Pacifici, P.G. & Witzemann, V., 2010. Differential muscle-driven synaptic remodeling in the neuromuscular junction after denervation. *The European journal of neuroscience*, 31(4), pp.646–58. Available at: http://www.ncbi.nlm.nih.gov/pubmed/20148944 [Accessed May 15, 2012].

Yoshimura, K. et al., 1999. The effect of reinnervation on force production and power output in skeletal muscle. *The Journal of surgical research*, 81(2), pp.201–8. Available at: http://www.ncbi.nlm.nih.gov/pubmed/9927541.

Zhang, J. et al., 2008. Magnetic resonance imaging of mouse skeletal muscle to measure denervation atrophy. *Experimental Neurology*, 212(2), pp.448–457.

Appendices

Appendix A: RNA integrity of all samples

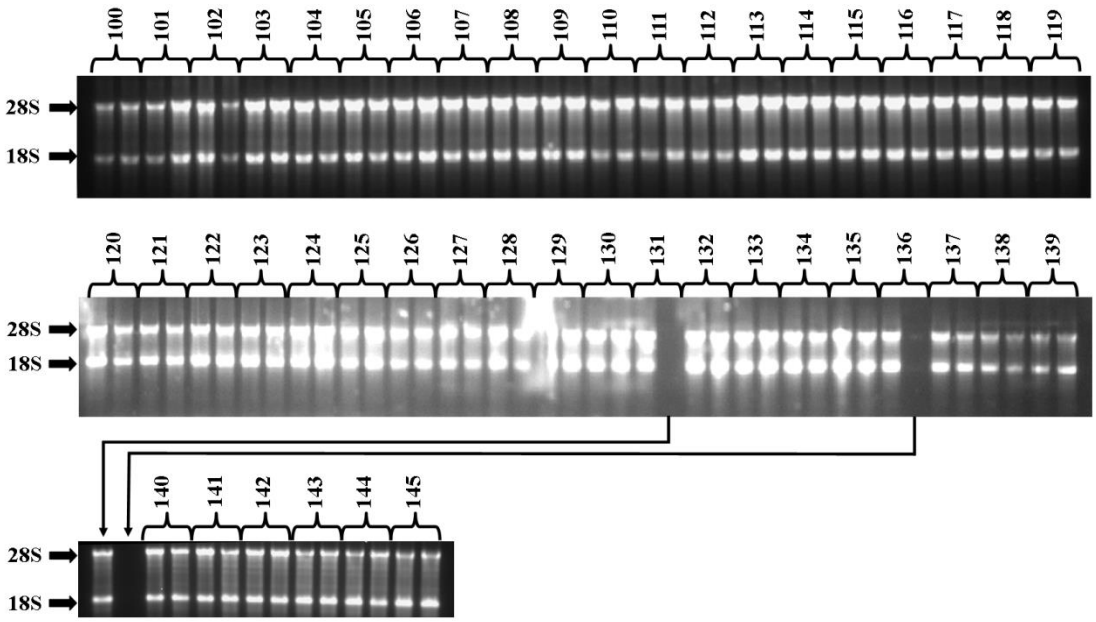

RNA integrity gels. Aliquots of each sample pair (denervated and sham; total of 45 samples subsequently processed for qPCR) were resolved on ethidium bromide stained agarose gels. For each animal ID (100 to 145), the first lane corresponds to the denervated (den) limb sample and the second lane corresponds to the contralateral control (sham). Clear 28S and 18S ribosomal RNA bands indicate samples that are free of RNA degradation. Two of the samples, 131-sham and 136-sham were not visible in their first run and are indicated by the long arrows. To determine if this was a loading error or some other type of experimental error, these two samples were resolved on a second gel. After the second run, 131-sham was detected but 136-sham sample was not. RNA was also undetectable for sample 136-sham after performing the spectrophotometric analysis. Animal 136 was therefore excluded from the qPCR analyses.

Appendix B: Comprehensive set of all western blot images

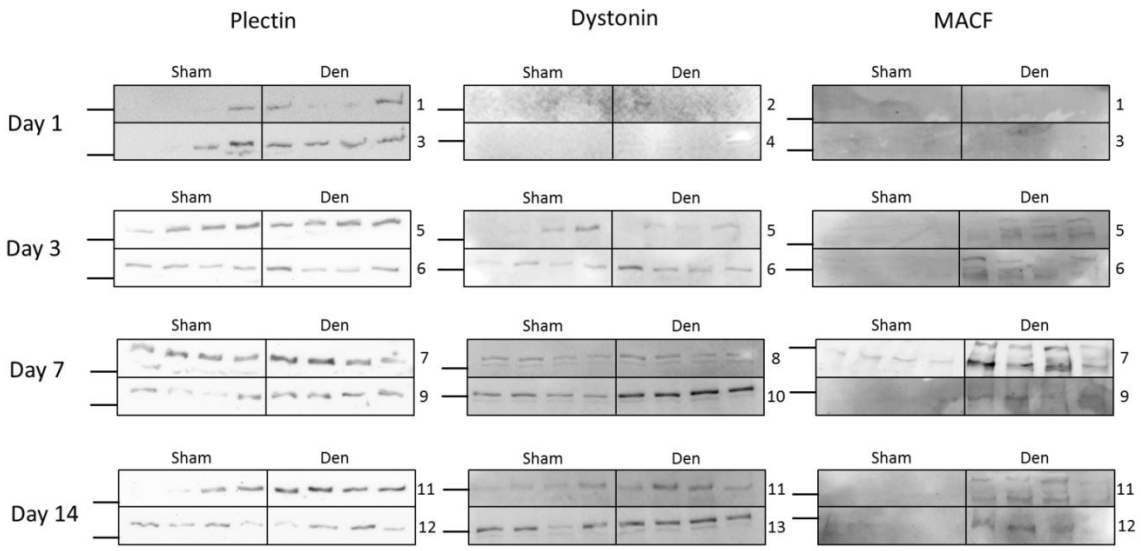

See methodology section for information on immunoblotting experiments. From left to right: plectin, dystonin and MACF blots and top to bottom: days 1, 3, 7 and 14. Numbers to the right of each blot correspond to the blot number (see Appendix C for corresponding coomassie-stained membranes). Lines to the left of the blots correspond to the 460kDa band of the HiMark protein ladder.

Appendix C: Coomassie stained membranes used for normalization

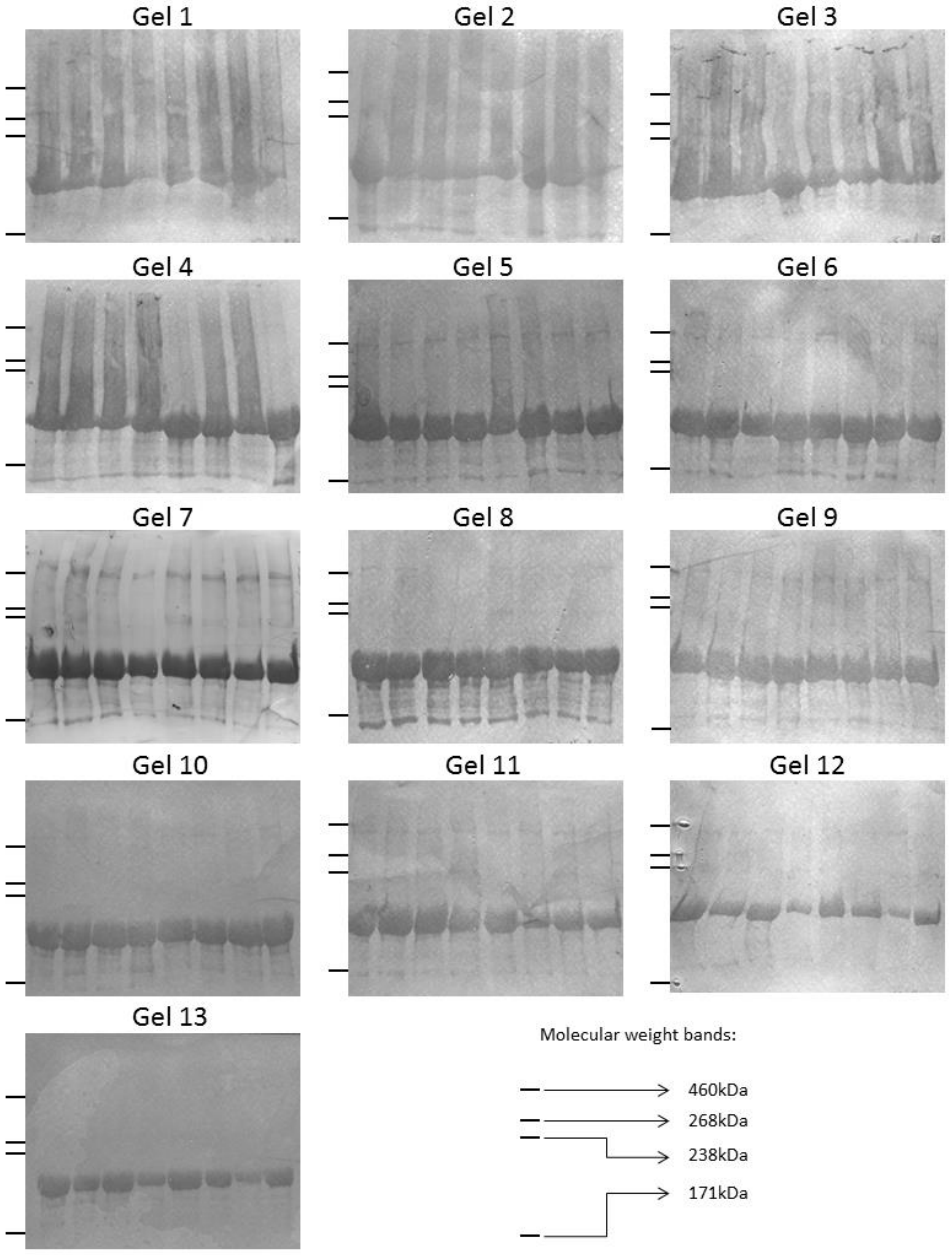

In total 13 membranes were used for the final analysis. At first immunoblotting experiments were attempted with 50ug of protein but the signal was very weak. We then used 100ug and determined that signal detection was significantly improved. The lines to the left of each gel represent molecular weight bands which, from top to bottom, correspond to 460, 268, 238 and 171kDa bands.

Appendix D: Animal Use Protocol certificate

LaurentianUniversity
UniversitéLaurentienne

TO: Céline Boudreau-Larivière

FROM: David MacLean

DATE: March 14, 2013

RE: AUP: 2013-03-02: Plakin expression in denervated mouse hind limb skeletal muscle

---

Dr. Boudreau-Larivière,

On March 13, 2013, the Animal Care Committee met to consider the above-mentioned AUP and voted to approve it.

Please provide a signed copy of the revised AUP to Pauline Zanetti (Research, Development and Creativity Office).

Sincerely,

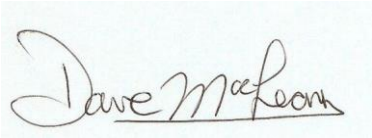

David MacLean, Ph.D.
Chair of the Animal Care Committee